

Q:1 *Compositional variation in
modern estuarine sands:
Predicting major controls on
sandstone reservoir quality*

Joshua Griffiths, Richard H. Worden, Luke J. Wooldridge,
James E. P. Utley, and Robert A. Duller

ABSTRACT

Primary depositional mineralogy has a major impact on sandstone reservoir quality. The spatial distribution of primary depositional mineralogy in sandstones is poorly understood, and consequently, empirical models typically fail to accurately predict reservoir quality. To address this challenge, we have determined the spatial distribution of detrital minerals (quartz, feldspar, carbonates, and clay minerals) in surface sediment throughout the Ravenglass Estuary, United Kingdom. We have produced, for the first time, high-resolution maps of detrital mineral quantities over an area that is similar to many oil and gas reservoirs. Spatial mineralogy patterns (based on x-ray diffraction data) and statistical analyses revealed that estuarine sediment composition is primarily controlled by provenance (i.e., the character of bedrock and sediment drift in the source area). The distributions of quartz, feldspar, carbonates, and clay minerals are primarily controlled by the grain size of specific minerals (e.g., rigid vs. brittle grains) and estuarine hydrodynamics. The abundance of quartz, feldspar, carbonates, and clay minerals is predictable as a function of depositional environment and critical grain-size thresholds. This study may be used, by analogy, to better predict the spatial distribution of sandstone composition and thus reservoir quality in ancient and deeply buried estuarine sandstones.

INTRODUCTION

Q:6 The composition of sandstone is primarily controlled by the geology of the hinterland, all the processes active between the sediment source area and the final site of deposition, with modification

AUTHORS

JOSHUA GRIFFITHS ~ *Department of Earth, Ocean and Ecological Sciences, University of Liverpool, Liverpool L69 3GP, United Kingdom; BP Exploration, Sunbury-on-Thames, Middlesex TW16 7LN, United Kingdom; joshua.griffiths@liverpool.ac.uk, joshua.griffiths@BP.com*

Joshua Griffiths completed this study as a postdoctoral research associate at the University of Liverpool, United Kingdom. Since, Joshua has moved to work as a geologist and reservoir quality specialist at BP Exploration, United Kingdom. His research interests focus on facilitating reservoir quality prediction in eolian, fluvial, and marginal marine sandstones. Joshua received his MSci in 2013 and Ph.D. in 2018 from the University of Liverpool.

RICHARD H. WORDEN ~ *Department of Earth, Ocean and Ecological Sciences, University of Liverpool, Liverpool L69 3GP, United Kingdom; rworden@liverpool.ac.uk*

Richard H. Worden is a professor of petroleum geology and geochemistry and leads the M.Sc. in petroleum reservoir geoscience at the University of Liverpool, United Kingdom. He gained his B.Sc. degree and his Ph.D. from Manchester University in the 1980s. Following a postdoctoral position in Edinburgh, Scotland, he worked for BP at their Sunbury-on-Thames site. He then took a lectureship at Queens University in Belfast, followed by a move to the University of Liverpool in 2000. His research interests include sandstone, mudstone, and carbonate petrology; diagenesis; reservoir quality; petrophysics and geochemistry; water-rock interaction; petroleum-rock interaction; thermochemical sulfate reduction; and the geology of CO₂ subsurface disposal.

LUKE J. WOOLDRIDGE ~ *Department of Earth, Ocean and Ecological Sciences, University of Liverpool, Liverpool L69 3GP, United Kingdom; BP Upstream Technology, Sunbury-on-Thames, Middlesex TW16 7LN, United Kingdom; luke90@liverpool.ac.uk*

Luke Wooldridge received his geology master's degree (MGeol [honours]) from the University of Leicester. His doctoral thesis was undertaken at the University of Liverpool and focused on establishing the origin of and a predictive

Q:2

Copyright ©2018. The American Association of Petroleum Geologists. All rights reserved.

Manuscript received January 26, 2018; provisional acceptance April 2, 2018; revised manuscript received June 27, 2018; final acceptance September 18, 2018.

DOI:10.1306/09181818025

framework for clay-coated grains in marginal marine systems. After his doctoral degree, Luke joined BP as a reservoir quality specialist. He has published five articles and coauthored four.

JAMES E. P. UTLEY ~ *Department of Earth, Ocean and Ecological Sciences, University of Liverpool, Liverpool L69 3GP, United Kingdom; etrsi@liverpool.ac.uk*

James E. P. Utley is a researcher in diagenesis, petroleum geology, applied mineralogy, and soils and clay mineralogy. He gained his master's in earth science at the University of Liverpool in 2008, remaining as a research assistant working on petrology, x-ray diffraction, and QEMSCAN[®] analysis. James currently works on research projects in reservoir quality assessment, CO₂ sequestration, and volcanology.

ROBERT A. DULLER ~ *Department of Earth, Ocean and Ecological Sciences, University of Liverpool, Liverpool L69 3GP, United Kingdom; rduller@liverpool.ac.uk*

Robert A. Duller is a lecturer in sedimentary geology at the University of Liverpool, United Kingdom. He gained his B.Sc. degree from the University of Leicester in 2002 and his Ph.D. from Keele University in 2007. In 2007, he took up a postdoctoral position at [CASP in Cambridge](#), and from 2008 to 2011 he was a research associate at Imperial College London. After a short research associate position at the University of Liverpool, he then took up the position of lecturer at the same institution in 2012. His research interests include sedimentation from catastrophic flow events, quantifying climatic and tectonic impacts on the sedimentary record, and the development of quantitative techniques for the field stratigrapher.

ACKNOWLEDGMENTS

This work was undertaken as part of the Chlorite Consortium at the University of Liverpool, sponsored by BP, Shell, Equinor, Eni, Chevron, Woodside, and Petrobras. We thank Barry Katz, Gemma Barrie, Stuart Jones, Christopher Stevenson, and one anonymous reviewer for their detailed and constructive comments that have helped improve this manuscript. Special thanks are offered to FEI (now Thermo Fisher Scientific)

potentially also happening during subsequent eo- and mesodiagenesis (Worden et al., 2018). Sandstone composition can be defined in terms of the proportions of quartz, feldspar, and lithics (QFL), the composition of the lithic fraction, the mineralogy of the matrix, and the amount of carbonate inherited from the initial depositional environment (Folk, 1968). Proportions of QFL and the amount of carbonate exert strong controls on reservoir quality (Primmer et al., 1997; Morad et al., 2010). The composition of sandstone may also significantly impact subsurface flow rates and influence wire-line log responses (e.g., sandstone density, natural radioactivity, electrical conductivity, and water saturation) and thus petrophysical properties (e.g., porosity, permeability, and wettability; Rider and Kennedy, 2011).

The porosity and permeability (reservoir quality) of a sandstone is initially controlled by sediment texture (i.e., grain size and sorting; Beard and Weyl, 1973; Scherer, 1987a, b). However, available statistical correlations typically fail to accurately predict reservoir quality, at least partly because the spatial variability of sandstone composition is poorly understood (Ajdukiewicz and Lander, 2010). The aim of this study is to map and analyze the spatial distribution of sediment texture (i.e., grain size and sorting) and composition (i.e., detrital quartz, feldspar, carbonates, and clay minerals) on a scale that is similar to many oil and gas reservoirs to aid reservoir quality prediction. This study is built upon the initial assumption that sandstone diagenetic systems are largely isochemical with respect to silicate minerals, although it is acknowledged that diagenetic processes that influence carbonate minerals may be somewhat more open system (Worden and Burley, 2003). The Ravenglass Estuary (Figure 1) was chosen for its accessibility, the varied hinterland geology, and because eo-genetic alterations are common in many shallow-marine and tidally influenced sandstone reservoirs (Morad et al., 2010). In addition, this work builds on the distribution of detrital clay coats in the Ravenglass Estuary (Wooldridge et al., 2017a, b, 2018).

The composition of a sandstone is typically described (by petrographers) in terms of the proportions of quartz, feldspar, and lithic grains, hence the use of Folk QFL ternary diagrams (Folk, 1968). Use of QFL diagrams may help define basin evolution, tectonic regime, and sediment supply over time (Dickinson and Suczek, 1979; Weltje, 2006); sediment transport routes (Caracciolo et al., 2012); and predict reservoir quality (Dutton and Loucks, 2010). Some petrographic studies have recognized that the behavior of lithic grains during compaction strongly varies depending on whether they are either ductile or rigid, with ductile behavior largely a function of the mineralogy of the lithic grain (Worden et al., 1997, 2000). The ductility of lithic grains is largely down to the proportion of clay minerals present; this led Ramm et al. (1997) and Ramm and Bjorlykke (1994) to use a clay mineral index, based on x-ray diffraction (XRD)-defined clay mineral and

Q:3

Q:4

Q:5

Q:7

82 mica quantities, to predict styles of compaction during sandstone
83 compaction. The quantity of carbonate minerals (primarily eo-
84 and mesogenetic cements) is also vitally important to reservoir
85 quality in many sandstones (Primmer et al., 1997; Morad et al.,
86 1998, 2010). Carbonate minerals are commonly inherited from
87 the specific sedimentary environment in which the sediment was
88 deposited—for example, bioclasts in marine sediments (Worden,
89 2006) and calcrete and dolocrete in arid, fluvial sediments (Schmid
90 et al., 2006).

Q:8

91 Because we have used XRD analysis, as opposed to petro-
92 graphy (which cannot quantify the mineralogy of clay-grade ma-
93 terial), in this modern analog study, the QFL end members have
94 here been recast. In this study, Q represents all types of quartz,
95 including mono- and polycrystalline quartz grains and quartz in
96 rigid, granitic and andesitic, lithic grains; F represents all feldspars,
97 including K-feldspar, plagioclase, perthite intergrowths, and any
98 feldspar minerals in granitic and andesitic volcanic lithic grains.

99 It is harder to define L in terms of XRD data, but here L has
100 been chosen to represent the sum total of all clay minerals, in-
101 dependent of grain size, including illite, chlorite, kaolinite, and
102 smectite. This is in accord with the study by Ramm et al. (1997)
103 that used clay mineral indices (including mica) for ductile com-
104 paction studies. The term “clay” refers to all sediment particles that
105 are smaller than 2 μm in size; in contrast, the term “clay mineral”
106 refers to aluminum-rich sheet silicate minerals. The name “illite”
107 in this study is independent of grain size and is used for micalike
108 minerals commonly associated with clastic sediments (e.g.,
109 muscovite) following the definition of Grim et al. (1937) (also
110 termed “illitic material” [Moore and Reynolds, 1997]).

111 A fourth term, C, represents carbonate minerals and has been
112 added since they have a major impact on reservoir quality and are,
113 in many cases, directly attributable to the specific depositional
114 environment; C therefore includes calcite, dolomite, aragonite,
115 and siderite. We therefore propose that XRD studies of sandstone
116 reservoir quality can be described in terms of QFL-C.

117 Sandstone composition in terms of QFL-C influences rock
118 properties in different ways at different times (e.g., during eo-
119 diagenesis and mesodiagenesis [Choquette and Pray, 1970]).
120 Eodiagenesis in sandstones occurs at temperatures less than ap-
121 proximately 60°C or 70°C, at which sediment can be influenced
122 by surface conditions and is in the biologically active zone (Morad
123 et al., 2000; Worden and Morad, 2003). Carbonate cements,
124 concretions, and nodules typically develop in sandstone during
125 eodiagenesis, and feldspar and lithic grain alterations typically
126 start during eodiagenesis (Worden et al., 2018).

127 Porosity and permeability of sandstones are initially controlled
128 by framework mineralogy (primarily the detrital quartz content),
129 matrix content, mean grain size, and sorting (Scherer, 1987a, b;
130 Ramm and Bjorlykke, 1994). We here discuss how QFL-C may

for providing the QEMSCAN, with huge
gratitude expressed to Alan Butcher for
facilitating this provision.

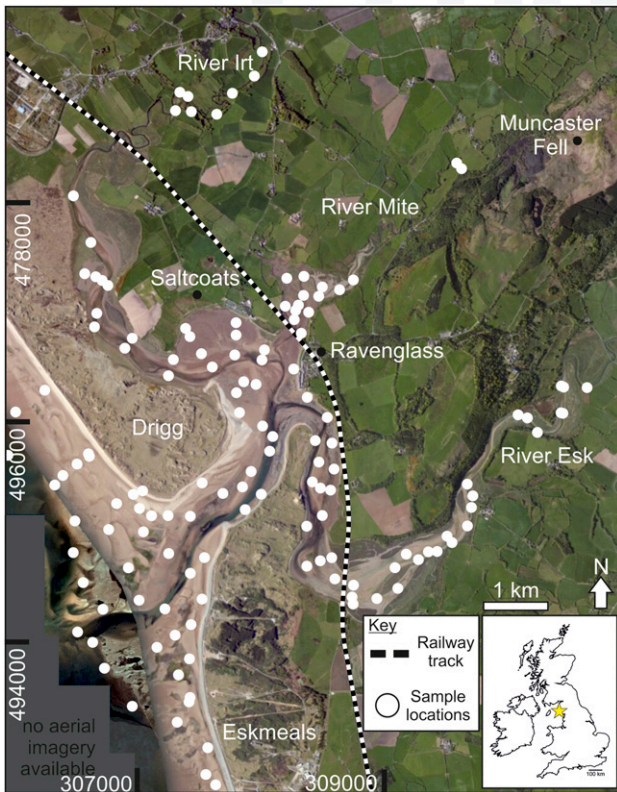


Figure 1. Aerial image (sourced from ArcGIS) of the Ravenglass Estuary, northwest England. Distribution of surface (<2 cm) sediment samples are highlighted by white circles.

impact sediment transport and deposition (and thus primary depositional mineralogy) and discuss the separate impacts of QFL-C during eodiagenesis and mesodiagenesis on the petrophysical properties (e.g., porosity, permeability, and wettability), composition, strength, and diagenetic reactivity of sandstones. The principles outlined below will be further addressed in the Discussion and Significance: Facilitating Sandstone Reservoir Quality Prediction during Petroleum Exploration, Appraisal, and Field Development and Production sections in relation to the specific results of this study and how they may facilitate reservoir quality prediction.

Sediment composition (QFL-C) may influence host-sediment properties (e.g., matrix content, mean grain size, sorting, and extent of detrital clay coat coverage) and thus impact sediment transport and deposition in the following ways. (1) Intergranular matrix material is typically enriched in clay minerals because of laws of hydrodynamics (Worden and Morad, 2003). (2) The proportion of quartz in sand may influence grain size because quartz grains are

relatively resistant to abrasion and are typically coarser than feldspar grains (Odom et al., 1976). (3) Weak framework grains (e.g., feldspar and clay-rich lithics) are likely to be reduced in size and promote wider grain-size distribution (Odom et al., 1976). (4) An abundance of clay minerals, in addition to biosediment interaction (presence of biofilms) in the top few millimeters of the primary depositional environment, may lead to the formation of detrital clay coats (Wooldridge et al., 2017a, b).

Sandstone composition (QFL-C) influences on eodiagenesis include the following. (1) Clay-rich ductile versus rigid grains, in which quartz-rich sediments undergo rigid compaction and phyllosilicate lithic- and mica-rich sediments undergo ductile compaction (Worden et al., 2000). (2) Weak versus strong grains, in which feldspar undergoes grain fracturing under lower tensile stresses than quartz grains (Rawling and Goodwin, 2003; Griffiths et al., 2018). (3) Reactive versus unreactive grains, in which feldspar, phyllosilicate, and carbonate tend to be relatively reactive in contrast to quartz, which is largely unreactive at temperatures less than 70°C to 80°C (Worden et al., 2000; Worden and Burley, 2003).

Sandstone compositional influences on mesodiagenesis are mainly controlled by the mineralogy of primary depositional and eodiagenetic grains, cement, and matrix. One of the major changes to reservoir quality in the mesodiagenetic realm is that exposed monocrystalline quartz surfaces and a suite of clay minerals become reactive at temperatures in excess of 70°C to 80°C (Worden and Burley, 2003; Worden and Morad, 2003). As a result, the following suite of mesodiagenetic processes are typical in sandstones. (1) Illite, chlorite, and dickite formation from precursor clay minerals and framework grains. (2) Albitization of plagioclase and K-feldspar, which may also lead to small amounts of carbonate and clay mineral cements (Chuhan et al., 2001; Worden and Burley, 2003; Morad et al., 2010). (3) Quartz grain pressure solution at grain contacts and subsequent quartz cementation, exacerbated by illite and mica (Oelkers et al., 1996; Meyer et al., 2006) or inhibited by chlorite or mixed-mineralogy chlorite-illite clay coats (Ehrenberg, 1993; Dowe et al., 2012; Saïag et al., 2016; Stricker and Jones, 2018). (4) Dissolution of unstable grains and calcite cements, which may enhance reservoir quality (Morad et al., 2010). In addition, throughout burial diagenesis, mineralogy is

Q:9

a big factor in determining the oil–water wetting preference of sandstones: for example, calcite, weathered feldspars, and Fe-rich chlorite are oil-wet minerals, whereas quartz, illite, and unweathered feldspars are water wet (Barclay and Worden, 2000).

The ability to predict sandstone composition would facilitate prediction of the petrophysical properties of sandstone reservoirs (e.g., porosity, permeability, and wettability) during petroleum exploration, appraisal, and field development and production. This study has focused on the modern Ravenglass Estuary in northwestern England, United Kingdom, by developing a unique modern analog of an estuarine sandstone and has addressed the following specific questions.

1. What minerals are found in the modern Ravenglass Estuary?
2. How are quartz, plagioclase, K-feldspar, carbonate, and clay minerals distributed in this modern estuarine setting?
3. What controls the whole-sediment mineral assemblage in a modern estuarine setting?
4. What controls mineral distribution patterns in estuarine environments?
5. Can the abundance and spatial distribution of sediment composition, and thus reservoir quality, be predicted as a function of grain size, depositional environment, and/or estuarine zone?

STUDY AREA: RAVENGLASS ESTUARY

The Ravenglass Estuary in northwestern England, United Kingdom, was chosen for this modern analog study because it has a similar area to many petroleum fields, was easy to access, is largely unmodified by the built environment, and has varied but well-studied hinterland geology. Furthermore, this study builds upon previous studies focused on detrital clay coat distribution in the Ravenglass Estuary (Wooldridge et al., 2017a, b, 2018).

Estuarine Hydrodynamics and Geomorphology

Q:10 The Ravenglass Estuary is a shallow, mixed-energy, and macrotidal (>7 m tidal range) estuarine system that occupies an area of 5.6 km² (3.5 mi²), of which approximately 86% is intertidal (Bousher, 1999;

Lloyd et al., 2013; Wooldridge et al., 2017b). Shallow estuary bathymetry has led to strong tidal asymmetry, resulting in the outward ebb tidal flow being prolonged in comparison with the inward tidal flow (Kelly et al., 1991). The discharge in the lower-Esk arm of the estuary during the ebb tidal flow (4.99 m³ s⁻¹ [16.37 ft³ s⁻¹]) is only slightly lower than flood tidal flow (5.41 m³ s⁻¹ [17.75 ft³ s⁻¹]) because of a short estuarine length (Kelly et al., 1991). Drigg and Eskmeals coastal spits provide shelter from wave action to the inner-estuarine zones and the central basin (Figures 2A, 3); however, strong tidal currents have resulted in extensive tidal bars and tidal dunes landward of the low-energy central minimum. The rivers flowing into the estuary have average flow rates of 0.4 m³ s⁻¹ (1.31 ft³ s⁻¹) for the River Mite, 3.4 m³ s⁻¹ (11.15 ft³ s⁻¹) for the River Irt, and 4.2 m³ s⁻¹ (13.78 ft³ s⁻¹) for the River Esk (Bousher, 1999). Anthropogenic impact on the estuary is here considered to be minor, excluding the sheltering of the inner Mite from tidal currents and increased salt marsh development as a consequence of the railway viaduct construction (Carr and Blackley, 1986).

Geological Setting

Sandstone compositions are largely controlled by the characteristics of the sediment's provenance, sedimentary processes active in the depositional basin, and sediment transport pathways that link provenance to basin, which is ultimately controlled by tectonic regime (Dickinson and Suczek, 1979). As a result, to assess the influence that provenance may have imposed on mineral type and distribution patterns in the Ravenglass Estuary, it is first necessary to identify the potential source of sediment mineral grains in the drainage basin. The type and spatial distribution of bedrock and drift deposits in the drainage basins of the Rivers Irt, Mite, and Esk are presented in Figure 2.

The northern River Irt drains Ordovician Borrowdale Volcanic Group andesites and the Triassic Sherwood Sandstone Group, whereas the River Esk predominantly drains the Devonian Eskdale Intrusions (Figure 2A). The Lower Triassic Sherwood Sandstone Group (locally known as the St Bees Sandstone Member) dominates the low-lying coastal planes and is predominantly composed of fluviatile sandstones

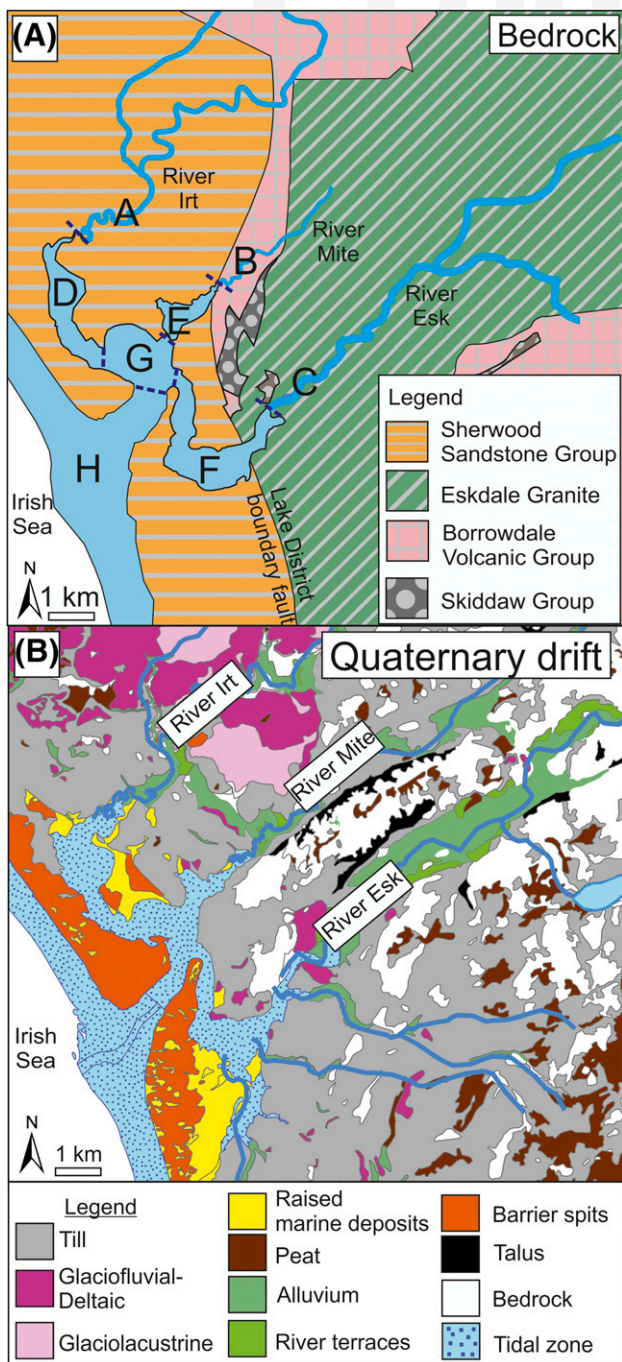


Figure 2. Geological setting of the Ravenglass Estuary, United Kingdom. (A) Bedrock geology (Ordovician Skiddaw Group and Borrowdale Volcanic Group, Devonian Eskdale Intrusions, and Triassic Sherwood Sandstone Group) and division of estuarine zones: lower Irt (A); lower Mite (B); lower Esk (C); inner Irt (D); inner Mite (E); inner Esk (F); central basin (G); and outer estuary (H). (B) Quaternary drift deposits.

(Quirke et al., 2015). The Borrowdale Volcanic Group, in the north of the provenance area, was subjected to subgreenschist facies metamorphism during the Caledonian orogeny (395 Ma) and is comprised of K-rich, calc-alkaline andesite (Quirke et al., 2015). The northern part of the Eskdale Intrusions, dominating to the east and south of the provenance area, is a coarse-grained granite, and the southern part is a granodiorite (Young et al., 1986). The Ordovician Skiddaw Group is comprised of weakly metamorphosed, fine-grained sedimentary rocks (Merritt and Auton, 2000) and is proximal to the Ravenglass Estuary (Figure 2A).

Quaternary drift deposits were deposited in response to spatially variable, glacio-isostatic rebound and glacio-eustatic sea-level change, following the last glaciation (late Devensian, ca. 28 to 13 ka) (Moseley, 1978; McDougall, 2001). However, much of the glacial deposit has since been eroded from the land surface (Merritt and Auton, 2000). The Seascale Glacigenic Formation (wide range of glacial and proglacial outwash sediments) is drained by the Rivers Irt, Esk, and Mite. The Gosforth Glacigenic Formation is primarily restricted to the northern River Irt and Mite drainage basin (Figure 2B). The Ravenglass Estuary is underlain by the Ravenglass Till Member (part of the Seascale Glacigenic Formation), which is locally exposed as knolls throughout the estuary.

SAMPLES AND METHODS

We undertook detailed ground surveys (aided by aerial imagery) and collected estuarine and drift deposit samples for grain-size and mineralogy analysis to assess the relationship between sediment composition, host-sediment properties (e.g., grain size), and depositional environment.

Field Mapping and Sample Collection

Aerial imagery and detailed ground surveys were used to define a suite of estuarine subenvironments. Sand abundance was used to subdivide tidal flats following the classification scheme proposed by Brockamp and Zuther (2004). According to this scheme, a sand flat has >90% sand, a mixed flat has 50%–90% sand, and

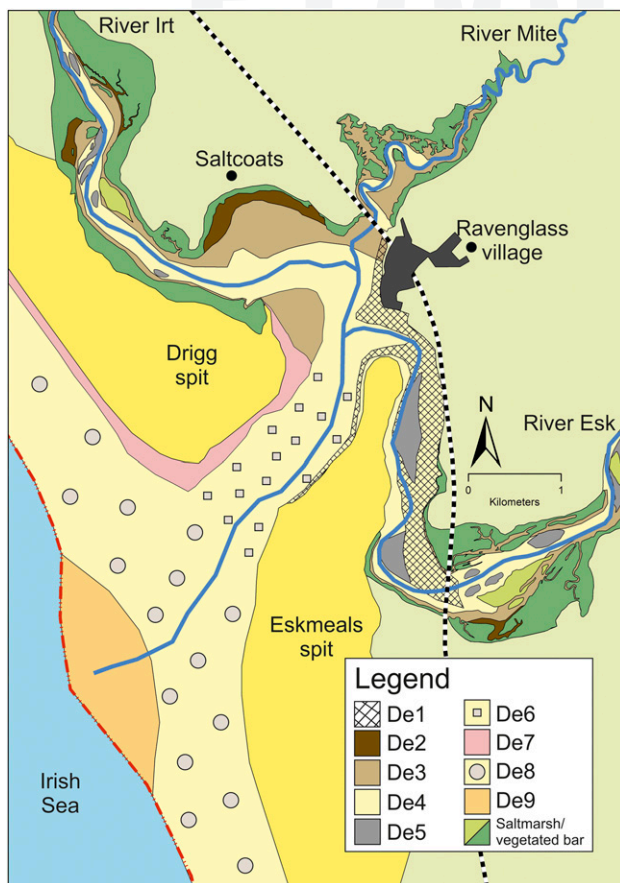


Figure 3. Nature and organization of depositional environments in the Ravenglass Estuary, labeled accordingly: gravel bed (De1); mud flat (De2); mixed flat (De3); sand flat (De4); tidal bars and dunes (De5); tidal inlet (De6); backshore (De7); foreshore (De8); and proebb delta (De9).

a mud flat has 15%–50% sand. Surface sediment samples ($n = 191$) were collected at low tide along predefined transects to give an approximately uniform distribution of estuarine and fluvial samples (Figure 1). Quaternary drift deposits were collected from exposed cliff sections in the inner Esk as well as from the Ravenglass Till Member, locally exposed as knolls throughout the estuary. Sediment samples were placed in airtight plastic jars in the field and stored in a refrigeration unit at approximately 2°C to prevent sample degradation prior to grain-size and mineralogical analyses. Mean grain size (microns), grain-size sorting (σ_g ; ~~higher values reflect more poorly sorted sediment~~), and sand abundance (percentage) were quantified using a Beckman Coulter laser particle size analyzer and GRADISTAT software (Blott and Pye, 2001). The grain-size sorting scale presented by Folk and Ward (1957) is here used,

in which high values are indicative of poorly sorted sediment. Grain-size sorting classes are as follows: 1.27–1.41 (well sorted), 1.41–1.62 (moderately well sorted), 1.62–2.0 (moderately sorted), 2.0–4.0 (poorly sorted), and 4–16 (very poorly sorted).

Clay Mineral Separation, Identification, and Quantification

X-ray Diffraction Analysis

To ensure accurate mineralogy identification and quantification (especially for chlorite, illite, mica, and kaolinite in the clay fraction of the sediment) and to analyze illite chemistry and crystallinity, clay fractions ($<2 \mu\text{m}$) and silt and sand fractions ($2 \mu\text{m}$ to 2mm) of estuarine sediment and Quaternary drift samples were physically separated prior to XRD analysis.

Clay fractions ($<2 \mu\text{m}$) were physically separated (isolated from the silt and sand fractions) in an ultrasonic bath, followed by gravity settling and then centrifuge settling at 5000 rpm for 10 min. The wet-separated clay fractions were then dried at 60°C for 24 hr and weighed to calculate the percentage of clay-size material. Dried clay fractions were crushed using a pestle and mortar prior to back-loading into cavity mounts and XRD analysis.

A representative 5-g subsample was taken from the separated silt and sand fractions ($2 \mu\text{m}$ to 2mm) and placed in an agate McCrone mill with 12 ml of distilled water and finely crushed for 10 min. The resultant slurry was washed into a petri dish using distilled water and then dried at 60°C. The dried material was crushed into a fine, loose powder using an agate pestle and mortar prior to back-loading into cavity mounts and XRD analysis to quantify the mineralogy of the silt and sand fractions ($2 \mu\text{m}$ to 2mm).

The mineralogy of the clay fraction ($<2 \mu\text{m}$) and silt and sand fraction ($2 \mu\text{m}$ to 2mm) was determined using a PANalytical X'Pert Pro MPD x-ray diffractometer. The XRD analyses were performed on randomly oriented powders, as opposed to oriented mounts, to achieve the precise (repeatable) quantification of all minerals, not just clay minerals. Mineralogy was determined by comparing acquired diffractograms with those in the International Centre for Diffraction Data Powder Diffraction File-2008 and with supplementary information from Moore and Reynolds (1997). The minerals were then quantified

using the relative intensity ratio method proposed by Chung, (1974a, b); results from this quantification method have been reported to be highly accurate (Hillier, 2000, 2003). The XRD results of the fine fraction (<2 μm) and silt and sand fraction (2 μm to 2 mm) were then recombined, factoring in the relative weight percentages of each size fraction to quantify the mineralogy of the whole sample (all material <2 mm).

The Esquevin index, which has previously been used to decipher sediment provenance (Gingele et al., 2001; Oliveira et al., 2002; Borchers et al., 2011; Bout-Roumazielles et al., 2013; Armynot du Châtelet et al., 2016), has been calculated (using clay fraction XRD data) to differentiate Al-rich from Fe–Mg-rich illite. An Esquevin index is calculated by analyzing the ratio between the 5 Å and 10 Å peak heights on x-ray diffractograms (Esquevin, 1969). High Esquevin indices indicate Al-rich illites (typically derived from chemically weathered rocks), whereas low Esquevin index values represent relatively Fe–Mg-rich illite (typically derived from physically eroded, unweathered rocks; Chamley, 1989). The following classification boundaries have been used in this study, after Esquevin (1969): biotite, less than 0.15 (most Fe–Mg rich); biotite + muscovite, 0.15–0.3; phengite, 0.3–0.4; muscovite, greater than 0.4 (most Fe–Mg depleted).

To establish illite crystallinity index ($2^{\circ}\theta$), also known as the Kübler index (Kübler, 1964), the full width at half maximum of the 10 Å (001) illite peak was measured on the x-ray diffractogram (using clay fraction XRD data). Highly crystalline illite is indicated by low illite crystallinity indices (narrow basal reflections), whereas poorly crystalline illite is indicated by high illite crystallinity indices (broad basal reflections) (Chamley, 1989). The following boundaries are used, after Kübler (1964): epizone (highest temperature), less than 0.25; anchizone, 0.25–0.42; diagenesis (lowest temperature), greater than 0.42.

Mineralogy of different-size fractions separated from a central basin (mixed-flat) sample was determined by XRD using a combination of gravity settling (as above) and sieving. The following grain-size classes were analyzed: less than 0.2 μm (fine clay); 0.2 to 2 μm (coarse clay); 2 to 32 μm (fine silt); 32 to 62 μm (coarse silt); 62 to 125 μm (very fine sand); 125 to 250 μm (fine sand).

Oil-wet mineral abundance was calculated as the sum total of oil-wet minerals, after Barclay and Worden

(2000): calcite, dolomite, kaolinite (assuming early alteration to kaolinite booklets), hematite, feldspar (assuming weathered; unweathered feldspars are water wet), and Fe-rich chlorite abundance. It is important to note that we have here assumed that (1) kaolinite will form kaolinite booklets during diagenesis and (2) that feldspars are weathered feldspar based on scanning electron microscope energy-dispersive spectrometer (SEM-EDS) results from Daneshvar and Worden (2018) in the Ravenglass Estuary.

~~Scanning Electron Microscope Energy Dispersive Spectrometer (QEMSCAN®)~~

Polished thin sections were constructed to provide textural and mineralogical information on detrital clay minerals (chlorite, illite, and kaolinite) to assess to what extent clay minerals occur as lithics and as part of the fine fraction (<2 μm). The SEM-EDS system employed in this study was an FEI Well Site QEMSCAN system, which is composed of a scanning electron microscope coupled with energy-dispersive spectrometers. QEMSCAN data provide information about the micron-scale texture and chemical and mineralogical composition. Data were collected with a step size of 2 μm to ensure both the fine fraction (<2 μm) and silt and sand fraction (>2 μm) were analyzed.

Spatial Mapping

Mineral distribution maps were made in ArcGIS® using an inverse distance weighted interpolation technique to avoid the creation of ridges or valleys of extreme and unrepresentative values (Watson and Philip, 1985). An interpolation barrier (polyline drawn in ArcGIS) along the long axis of Drigg and Eskmeals spits was used to ensure interpolated values on either side of the spits (i.e., in the estuary and on the coast) did not influence one another despite their relative spatial proximity.

Statistical Analysis

An analysis of variance (ANOVA) test was used to assess whether there is a statistically significant difference in abundance of specific minerals as a function of depositional environment (De1 to De9) and

estuarine zone (A–H). Following ANOVA, a post hoc Tukey’s honestly significant difference (HSD) test (Odeh and Evans, 1974; R Core Team, 2016) was employed to determine which individual depositional environment or estuarine zones were statistically different from one another as a function of specific mineral abundance (quartz, feldspar, clay minerals, and carbonate). The following symbols were used to highlight statistical significance (*p* value); marginally significant (+) when the *p* value was <0.1; significant (*) when the *p* value was <0.05; very significant (**) when the *p* value was <0.01; and extremely significant (***) when the *p* value was <0.001. All statistical analyses were performed in R statistical software (R Core Team, 2016).

RESULTS

In this section, we present results from detailed ground surveys (aided by aerial imagery) undertaken to identify the nature and distribution of the depositional environment as well as results from laboratory analyses used to quantify sediment properties (grain size, sorting, and mineralogy).

Estuarine Sediment Characteristics

The estuary has been subdivided into discrete fluvial, inner, central, and outer zones (Figure 2A) based upon reported salinity data and the dominant physical processes active in each zone (Assinder et al., 1985; Daneshvar, 2015). Zones A to C represent fluvial (river) regions that are freshwater dominated; zones D to F (inner) represent brackish, inner river- and tide-dominated regions; zone G (central) is a relatively mixed-energy (fluvial-, tide-, and wave-influenced) and heterogeneous central zone with near-seawater salinity that contains extensive mud flat and mixed flat (locally named Saltcoats tidal flat); and zone H (outer) is seawater dominated and subject to strong wave and tidal currents.

The mapped distribution of nine discrete depositional environments are presented and explained in Figure 3.

The average grain size and grain-size sorting of each depositional environment and estuarine zone are presented in Tables 1 and 2. The mapped distributions of grain size and grain sorting are presented Figure 4. Variation in grain size and grain sorting for each

estuarine zone and depositional environment are displayed in Figure 5 and Tables 1 and 2.

Estuarine Composition

Here, XRD studies, as opposed to petrographic techniques, have been used to quantify mineralogy. It is therefore not possible to create traditional QFL ternary diagrams, which are typically used to classify sandstones (Folk, 1954) or in provenance studies (Dickinson and Suczek, 1979). However, our SEM-EDS analyses have revealed that clay minerals, especially chlorite, occur in the silt- and sand-size fraction as lithic fragments as well in the clay fraction of the sediment (Figure 6A). As a result, XRD-QFL ternary plots (Figure 7) closely compare with traditional petrographic QFL plots and reveal the relative abundance of quartz, feldspar, and lithic grains that are enriched in clay minerals. Figure 7 reveals that the relative abundance of QFL varies as a function of estuarine zone.

Composition of Drift Deposits

Data on XRD have been produced from (1) drift deposits exposed in the cliff sections in the inner Esk (Gosforth Glaciogenic Formation and Seascale Glaciogenic Formation) and (2) the Ravenglass Till Member (part of the Seascale Glaciogenic Formation). Ravenglass Till Member samples (*n* = 3) have the following mineral assemblage: quartz (65%–75%), plagioclase (8%–14%), K-feldspar (6%), chlorite (2%–3%), illite (6%–8%), and kaolinite (5%). The Ravenglass Till Member is dominated by well-crystalline, Fe–Mg-enriched illite (Esquevin index: 0.28; illite crystallinity: 0.24). The Fishgarth Wood Till Member (part of the Gosforth Glaciogenic Formation) (*n* = 1) has the following mineral assemblage: quartz (81%), plagioclase (7%), K-feldspar (6%), chlorite (<0.5%), illite (5%), and kaolinite (1%). The Fishgarth Wood Till Member is dominated by Al-enriched illite (Esquevin index: 0.43; illite crystallinity: 0.21).

Mineral Abundance and Grain-Size Fraction

To determine whether different minerals are preferentially most abundant within different grain-size

Table 1. Summary of the Mineralogy (Mean and Standard Deviation), Host Sediment Properties (Mean Grain Size and Sorting), and Oil-Wet Mineral Abundance (Percentage) of the Nine Depositional Environments, Including Weighted Averages

	Depositional Environment										W.AV
	De1	De2	De3	De4	De5	De6	De7	De8	De9	De9	
	Number of Samples, <i>n</i>										
Quartz, mean (sd)	78.62 (8.48)	71.50 (5.83)	77.78 (6.83)	86.15 (1.33)	85.10 (3.24)	85.40 (2.35)	86.66 (0.02)	85.04 (2.54)	86.32 (0.79)	86.32 (0.79)	82.06
Plagioclase, mean (sd)	9.98 (3.47)	11.31 (1.99)	9.45 (2.35)	7.42 (0.98)	8.17 (1.71)	7.29 (0.85)	6.25 (0.57)	7.19 (1.49)	7.35 (0.80)	7.35 (0.80)	8.35
K-feldspar, mean (sd)	5.51 (0.55)	5.45 (0.47)	5.84 (0.96)	5.00 (0.79)	4.85 (0.85)	4.73 (1.05)	5.58 (0.57)	5.38 (0.86)	4.66 (0.72)	4.66 (0.72)	5.39
Carbonate, mean (sd)	2.00 (1.31)	2.84 (1.12)	2.06 (0.85)	0.88 (0.42)	0.54 (0.51)	1.03 (0.70)	0.50 (0.01)	1.08 (0.72)	0.99 (0.09)	0.99 (0.09)	1.43
Chlorite, mean (sd)	1.56 (1.73)	2.33 (1.13)	1.19 (1.23)	0.21 (0.57)	0.67 (1.16)	0.66 (0.60)	0.50 (0.00)	0.54 (0.40)	0.36 (0.37)	0.36 (0.37)	0.87
Illite, mean (sd)	2.24 (2.69)	5.50 (3.19)	2.98 (2.68)	0.25 (0.24)	0.55 (0.96)	0.68 (0.69)	0.51 (0.01)	0.62 (0.74)	0.23 (0.27)	0.23 (0.27)	1.62
Kaolinite, mean (sd)	0.09 (0.06)	1.06 (0.86)	0.68 (0.64)	0.09 (0.08)	0.12 (0.26)	0.12 (0.18)	0.01 (0.00)	0.06 (0.16)	0.01 (0.00)	0.01 (0.00)	0.31
Mean grain size, μm	370 (110)	39 (11)	115 (56)	253 (90)	283 (109)	312 (88)	324 (32)	291 (101)	239 (84)	239 (84)	225
Grain-size sorting, σg	1.86 (0.44)	3.54 (0.82)	2.37 (0.66)	1.59 (0.53)	1.59 (0.52)	1.53 (0.31)	1.35 (0.02)	1.44 (0.14)	1.48 (0.34)	1.48 (0.34)	1.90
Oil-wet M. abundance, %	19.1 (5.86)	23 (3.66)	19.21 (4.43)	13.6 (1.2)	14.36 (2.61)	13.91 (1.99)	12.83 (0.01)	14.33 (2.12)	13.44 (0.71)	13.44 (0.71)	16.31

Oil-wet mineral abundance is the sum total of calcite, dolomite, kaolinite (assuming early alteration to kaolinite booklets), hematite, feldspar (assuming weathered; unweathered feldspars are water wet), and Fe-rich chlorite abundance, after Barclay and Worden (2000). Depositional environments are labeled accordingly: gravel bed (De1); mud flat (De2); mixed flat (De3); sand flat (De4); tidal bars and dunes (De5); tidal inlet (De6); backshore (De7); foreshore (De8); and proebb delta (De9).

Abbreviations: M. = mineral; NA = xxx; sd = standard deviation; W.AV = weighted average.

Q:56

Q:57

Q:58

Table 2. Summary of the Mineralogy (Mean and Standard Deviation), Host Sediment Properties (Mean Grain Size and Sorting), and Oil-Wet Mineral Abundance (Percentage) of the Eight Estuarine Zones, Including Weighted Averages **Q:59**

	Estuarine Zone								W.Av	Clay Index of W.Av
	A	B	C	D	E	F	G	H		
	11	2	10	19	19	34	28	68		
Quartz, mean (sd)	75.97 (3.28)	77.88 (1.42)	67.60 (11.11)	78.84 (5.84)	74.44 (7.76)	82.54 (6.00)	81.10 (7.60)	85.36 (2.30)	80.95	
Plagioclase, mean (sd)	11.93 (1.64)	12.01 (0.00)	14.57 (6.81)	10.05 (2.17)	10.53 (2.64)	8.40 (2.21)	8.20 (1.85)	7.21 (1.31)	8.89	
K-feldspar, mean (sd)	6.53 (0.47)	6.50 (0.70)	6.86 (1.85)	5.57 (1.36)	6.01 (0.88)	5.18 (0.65)	5.41 (0.88)	5.17 (0.91)	5.51	
Carbonate, mean (sd)	0.12 (0.35)	0.00 (0.00)	0.22 (0.28)	1.76 (1.20)	2.09 (1.01)	1.34 (1.08)	1.81 (1.01)	1.03 (0.65)	1.27	
Chlorite, mean (sd)	1.50 (0.87)	1.52 (0.71)	3.43 (1.74)	1.20 (1.23)	1.87 (1.42)	0.82 (1.18)	0.78 (1.17)	0.53 (0.42)	1.04	0.31
Illite, mean (sd)	3.46 (1.56)	2.05 (1.41)	5.95 (2.77)	2.15 (2.24)	4.18 (3.00)	1.41 (2.01)	2.22 (3.19)	0.56 (0.67)	1.94	0.58
Kaolinite, mean (sd)	0.46 (0.77)	0.03 (0.00)	1.35 (1.55)	0.40 (0.31)	0.86 (0.77)	0.29 (0.51)	0.49 (0.69)	0.06 (0.15)	0.37	0.11
Mean grain size, μm	190 (120)	539 (19)	213 (234)	202 (159)	90 (71)	221 (123)	184 (107)	291 (96)	227	x
Grain-size sorting, σg	2.53 (0.69)	1.53 (0.07)	2.79 (1.14)	2.30 (0.87)	2.47 (0.68)	1.86 (0.69)	2.31 (1.10)	1.45 (0.21)	1.97	
Oil-wet M. abundance, %	20.58 (2.37)	20.07 (NA)	26.45 (9.87)	18.97 (4.00)	21.36 (5.06)	16.03 (4.16)	16.67 (4.62)	14.06 (1.92)	17.10	

Estuarine zones are labeled accordingly: lower Irt (A); lower Mite (B); lower Esk (C); inner Irt (D); inner Mite (E); inner Esk (F); central basin (G); and outer estuary (H). Abbreviations: M. = mineral; W.Av = weighted average.

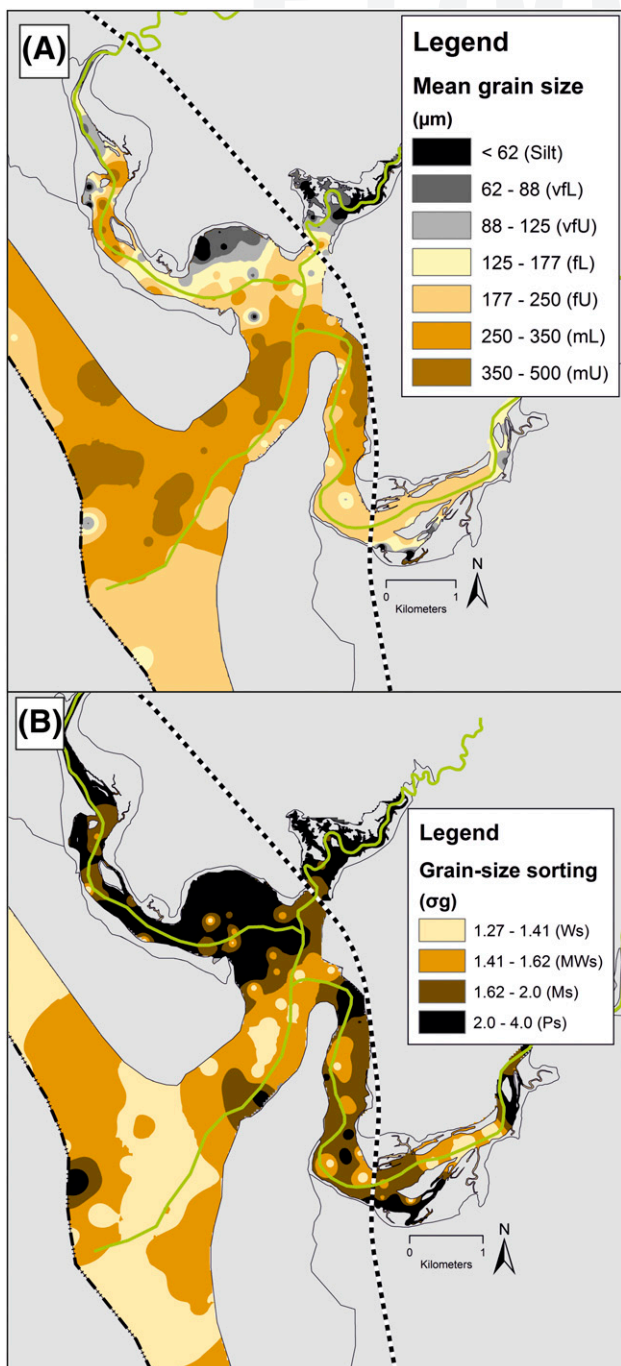


Figure 4. Distribution of host sediment properties: (A) mean grain size and (B) grain-size sorting. Note that textural maturity and mean grain size decrease toward the margins of the inner estuary and central basin. Mean grain-size classes are labeled accordingly: silt; lower very fine sand (vfl); upper very fine sand (vfU); lower fine sand (fl); upper fine sand (fU); lower medium sand (mL); and upper medium sand (mU). Grain-size sorting classes are labeled accordingly: well sorted (Ws); moderately well sorted (MWs); moderately sorted (Ms); and poorly sorted (Ps).

fractions, a whole-sediment sample from the Saltcoats mixed flat was split into grain-size fractions and analyzed using XRD. The proportion of minerals in each grain-size fraction is shown in Figure 8A. Quartz abundance increases with an increase in grain size (Figure 8A). The K-feldspar abundance appears to be independent of grain size (Figure 8A). Plagioclase is most abundant in fine to coarse silt-size sediment (~2 to ~63 µm; Figure 8A). The abundance of clay minerals (chlorite, illite, and kaolinite) and carbonate (mostly calcite) decreases with an increase in grain size (Figure 8A).

Chlorite, illite, kaolinite, and smectite abundance have been plotted as a function of grain-size fraction to assess if the relative abundance of specific clay minerals varies between grain-size fractions (Figure 8B). Relative chlorite abundance typically increases with an increase in grain size; the relative abundance of illite and kaolinite decreases with an increase in grain size (Figure 8B). Smectite abundance is negligible and is largely restricted to ~~size sediment~~ **Q:18** ~~fractions less than 15 µm~~ (Figure 8B).

Mapped Estuarine Mineral Distribution

The mapped distributions of quartz, plagioclase, K-feldspar, and carbonate are presented in Figure 9. Quartz abundance ranges from 64% to 90% and typically increases in abundance toward the open sea (Figure 9A). Quartz is most abundant (~90%) in outer-estuarine (tidal inlet, foreshore, and backshore) sediment and least abundant (~64%) toward the margin of the inner estuary and the central basin (Figure 9A).

Plagioclase abundance ranges from 6% to 15% and increases in abundance with proximity to the fluvial-marine interface and toward the margin of the inner estuary and central basin (Figure 9B). Variations in K-feldspar abundance (3%–8%) are relatively minor throughout the Ravenglass Estuary, but there is a minor reduction in K-feldspar abundance in tidal inlet and northern foreshore sediment (Figure 9C).

Carbonate abundance ranges from 0% to 5% (of which >95% is calcite, <5% is aragonite, and <1% is dolomite) and increases in abundance toward the margin of the inner estuary and central basin (Figure 9D). Carbonate material is least abundant upon the northern foreshore and in the tidal inlet (Figure 9D).

The mapped distributions of clay fraction abundance and abundance of specific clay minerals are

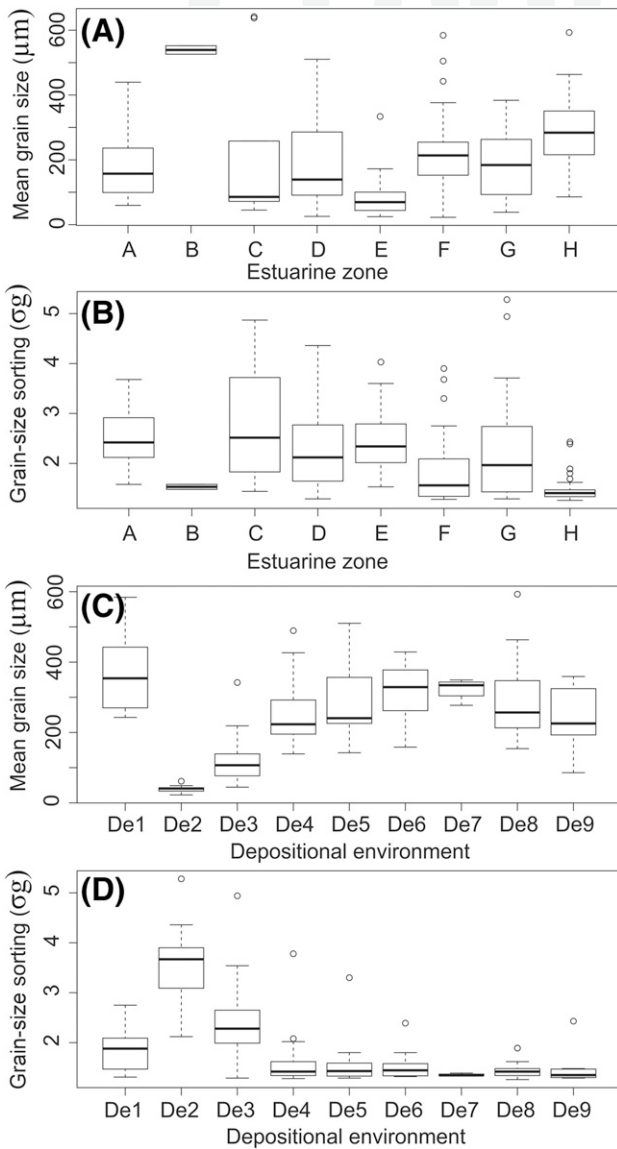


Figure 5. Host sediment properties as a function of estuarine zone and depositional environment. (A) Mean grain size as a function of estuarine zone, (B) grain-size sorting as a function of estuarine zone, (C) mean grain size as a function of depositional environment, and (D) grain-size sorting as a function of depositional environment. Grain-size sorting classes are as follows: 1.27–1.41 (well sorted [Ws]); 1.41–1.62 (moderately well sorted [MWs]); 1.62–2.0 (moderately sorted [Ms]); 2.0–4.0 (poorly sorted [Ps]); and 4–16 (very poorly sorted [VPs]). Note that textural maturity and mean grain size decrease toward the margins of the inner estuary and central basin (i.e., in mud flats and mixed flats). Estuarine zones are labeled accordingly: lower Irt (A); lower Mite (B); lower Esk (C); inner Irt (D); inner Mite (E); inner Esk (F); central basin (G); and outer estuary (H). Depositional environments are labeled accordingly: gravel bed (De1); mud flat (De2); mixed flat (De3); sand flat (De4); tidal bars and dunes (De5); tidal inlet (De6); backshore (De7); foreshore (De8); and proebb delta (De9). Note that outliers (open circles) are defined as an

displayed in Figure 10. Clay-size material is most abundant toward the estuarine margins in the inner estuary and the central basin and is negligible in the outer estuary (<0.5%). Chlorite is most abundant in Saltcoats tidal flat sediment and has a relatively patchy distribution throughout the inner estuary zones (Figure 10B). Illite is most abundant in Saltcoats tidal flat and has a relatively patchy distribution throughout the inner estuary zones (Figure 10C). Kaolinite, of minor abundance, is predominantly found in mud flats (Figure 10D).

Mineral Abundance versus Mean Grain Size

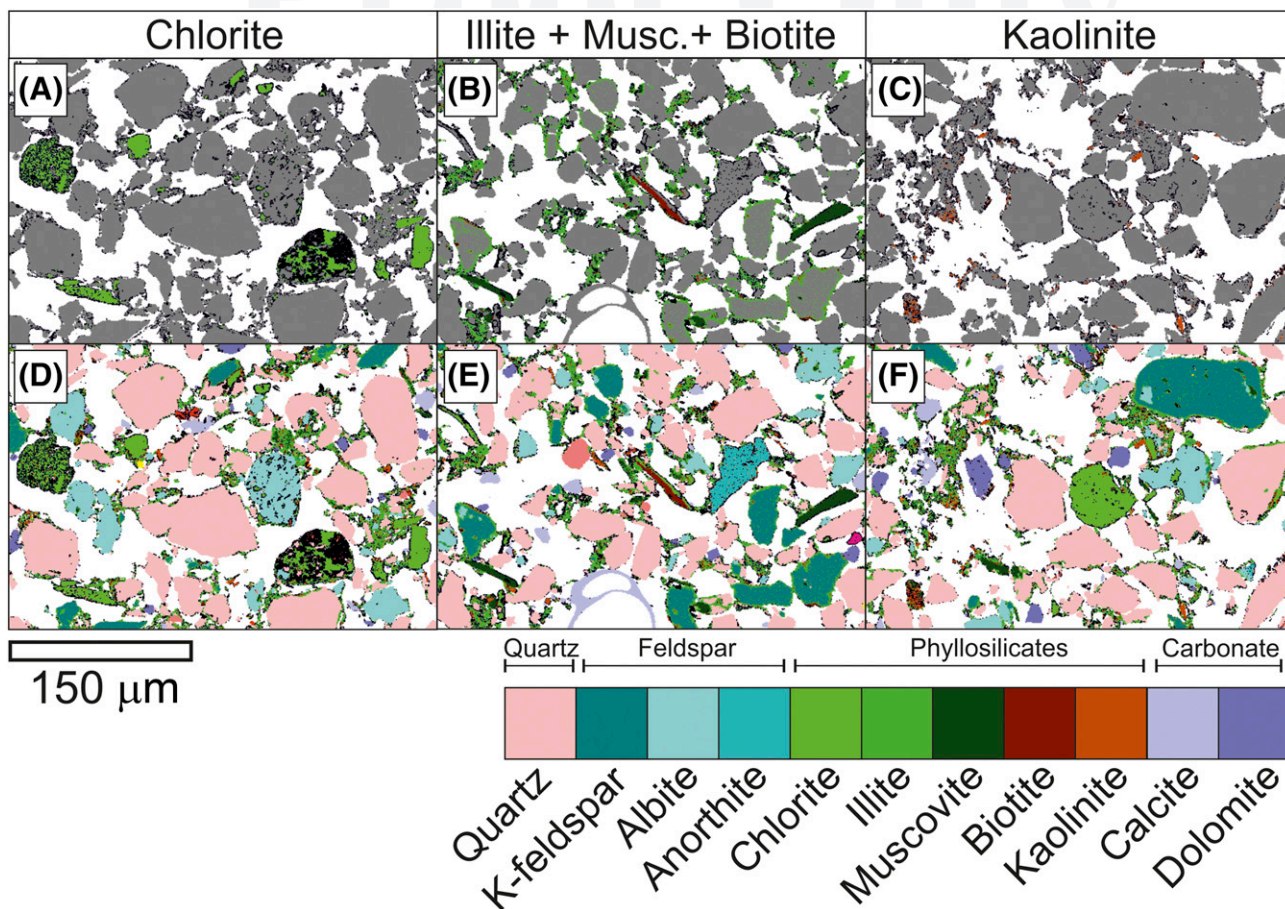
The relationships between mean grain size and the abundance of quartz, K-feldspar, plagioclase, and carbonate, as a function of depositional environment, are presented in Figure 11.

Quartz has uniformly high abundance (~85%) in sediment between upper fine sand (>177 µm) and medium upper sand (<350 µm). Between the grain-size classes silt to upper fine sand (62–177 µm), in mixed-flat sediments, quartz abundance typically increases with an increase in mean grain size (Figure 11A). Gravel beds have a wide range of quartz abundance (Figure 11A). Note that quartz abundance in mud flats is relatively low (~65%–80%) but does not correlate to mean grain size.

Between the grain-size classes silt to upper very fine sand (62–125 µm), plagioclase abundance typically decreases with an increase in mean grain size (Figure 11B). Plagioclase has lower abundance (~6%–8%) in sediment between upper fine sand and medium upper sand (125–350 µm). Gravel beds have a wide range of plagioclase abundance (Figure 11B). Note that plagioclase abundance in mud flats is relatively high (~8%–14%) but does not correlate with mean grain size.

With an increase in mean grain size, there is a subtle reduction in K-feldspar abundance (Figure 11C); the highest abundance is found in some mixed-flat sediments (7%–8%), and the lowest abundance is found in sediment with a grain size greater than 350 µm in tidal inlets and the foreshore (3%–4%). However, most depositional environments have a K-feldspar abundance of approximately 5%–6%.

Figure 5. Continued. observation that is numerically distant from the rest of the data (i.e., a value that is 1.5 times the interquartile range below the lower quartile and above the upper quartile).



Q:52 Figure 6. Scanning electron microscope energy dispersive spectrometer (SEM-EDS) analyzing the micron-scale (2- μ m) texture and chemical and mineralogical composition of a single central basin sample. (A-C) The textural characteristics of chlorite, illite, biotite, and kaolinite are shown. Only the clay minerals chlorite, illite, or kaolinite are colored. (D-F) The textural characteristics of all framework grains and matrix minerals are shown. All minerals are colored. Note that lithic fragments are typically chlorite rich. Musc. = muscovite.

Q:53

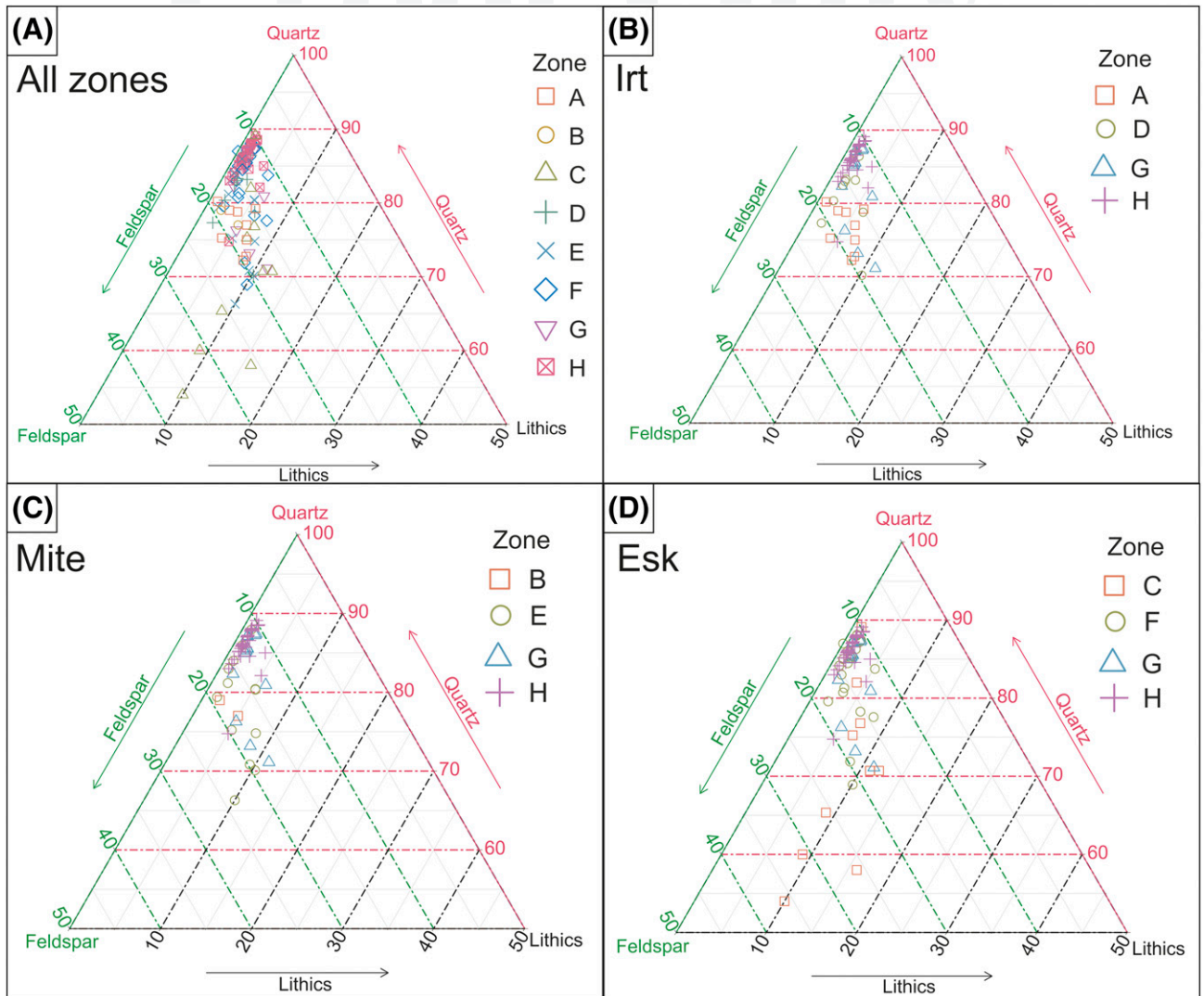
Between the grain-size classes silt to upper fine sand (primarily mixed flats), carbonate abundance typically increases with a reduction in mean grain size (Figure 11D). Carbonate is most abundant (~2%–4%) in sediment that has a mean grain size less than upper fine sand (177 μ m; Figure 11D). Carbonate abundance is relatively uniform (~1%) in sediment that has a grain size greater than upper fine sand (177 μ m). Gravel beds and mud flats have a wide range of carbonate abundance that shows no relationship to grain size (Figure 11D).

The relationships between mean grain size and the abundance of clay fraction in estuarine sediments as well as the abundance of specific clay minerals (chlorite, illite, and kaolinite), as a function of depositional environment, are presented in Figure 12.

Clay fraction abundance decreases with mean grain size in sediment up to upper fine sand (177 μ m;

Figure 12A). Clay fraction abundance is uniform (typically <1%) in sediment coarser than 177 μ m. Clay fraction is most abundant in mud flats and mixed flats; all other depositional environments (De3 to De9) typically contain low concentrations of clay-size material (typically <1%).

Chlorite abundance typically decreases with an increase in mean grain size, with a sharp decrease in chlorite abundance in sediment that has a mean grain size greater than lower very fine sand (88 μ m; Figure 12B). Elevated chlorite concentrations also occur in some foreshore, tidal inlet, tidal dune, and tidal bar sediments (Figure 12B). Chlorite abundance typically increases with an increase in grain size in tidal inlet (De6) and foreshore sediment (De8; Figure 12B). Gravel beds and mud flats have a wide range of chlorite abundance that shows no relationship to grain size (Figure 12B).



Q:54 Figure 7. X-ray diffraction quartz, feldspar, and lithics (QFL) ternary plots; lithics are here defined as the sum total of clay minerals (chlorite, illite, kaolinite, and smectite) in the silt and sand fraction. (A) The QFL distribution throughout all estuarine zones; (B) River Irt, inner Irt, central basin, and outer-estuarine composition; (C) River Mite, inner Mite, central basin, and outer-estuarine composition; (D) River Esk, inner Esk, central basin, and outer-estuarine composition. Note that River Esk sediment is relatively feldspathic and enriched in lithics (most likely chlorite). Estuarine zones are labeled accordingly: lower Irt (A); lower Mite (B); lower Esk (C); inner Irt (D); inner Mite (E); inner Esk (F); central basin (G); and outer estuary (H).

Illite abundance typically decreases with an increase in mean grain size (Figure 12C). A sharp increase in illite abundance is observed in sediment with a mean grain size of less than lower very fine sand (88 μm) (Figure 12C). Illite abundance is typically low (<2%) and shows no relationship with mean grain size in sediment that is coarser than upper fine sand (177 μm) (Figure 12C). Gravel beds and mud-flats have a wide range of illite abundance that shows no relationship to grain size (Figure 12C).

In mud flats and mixed flats, there is a minor decrease in kaolinite abundance (1%–3%) with increasing mean

grain size (Figure 12C). The majority of depositional environments show kaolinite abundance is minor (<1%) and has no relationship with mean grain size.

Illite Composition and Crystallinity versus Mean Grain Size

The clay mineral assemblage of the Ravensglass Estuary is dominated by Fe–Mg-rich illite (Figures 10D, 13A). Illite composition and crystallinity have been plotted against mean grain size as a function of

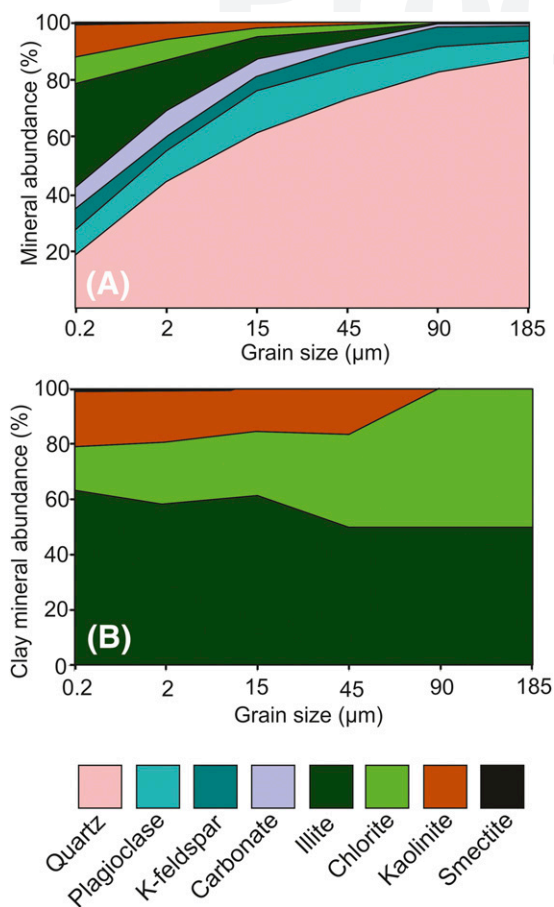


Figure 8. Relative abundance of specific minerals as a function of grain-size class, extracted from a singular disaggregated (e.g., clay minerals removed from the surface of sand grains) central basin whole-sediment sample. (A) Whole mineral assemblage. (B) Relative proportions of chlorite, illite, kaolinite, and smectite. Note that chlorite is relatively most abundant in coarser-grained sediment in comparison with illite, kaolinite, and smectite.

in Tables 1 and 2 as well as the relative abundance of each clay mineral (e.g., chlorite/[chlorite + illite + kaolinite]) for the entire estuary. Box-and-whisker plots display the ranges and standard deviations as well as the median values for each specific mineral as a function of depositional environment and estuarine zones (Figures 14, 15). The abundance of preferentially oil-wet minerals (calcite, dolomite, kaolinite, hematite, Fe-rich chlorite, and weathered feldspar) per depositional environment and estuarine zone is presented in Tables 1 and 2 and displayed as box-and-whisker plots in Figure 15G, H.

The ANOVA results show that there is a statistically significant difference ($p < 0.05$) in relative mineral abundance as a function of both estuarine zone and depositional environment. The multicomparison, post hoc Tukey HSD results reveal statistical differences ($p < 0.05$) in mineral abundance between paired estuarine zones and depositional environments (Tables 3–6).

DISCUSSION

Controls on the composition (mineral assemblage) of the Ravenglass Estuary as well as the controls on QFL-C distribution patterns are discussed in this section. Influences on mineral distribution patterns that are here discussed include provenance and sediment transport pathways, estuarine hydrodynamics, and early diagenesis (both in situ diagenesis and continued mineral alteration during sediment transport).

Controls on Estuarine Sediment Composition

In the Ravenglass Estuary, there are three potential sources of sediment: (1) fluvial drainage of bedrock in the hinterland (Figure 2A); (2) fluvial drainage and local erosion of drift and soil deposits in the hinterland, underlying the estuary and exposed in proximal cliff sections (Figure 2B); and (3) marine inundation with landward displacement of littoral-zone sediment into the estuary.

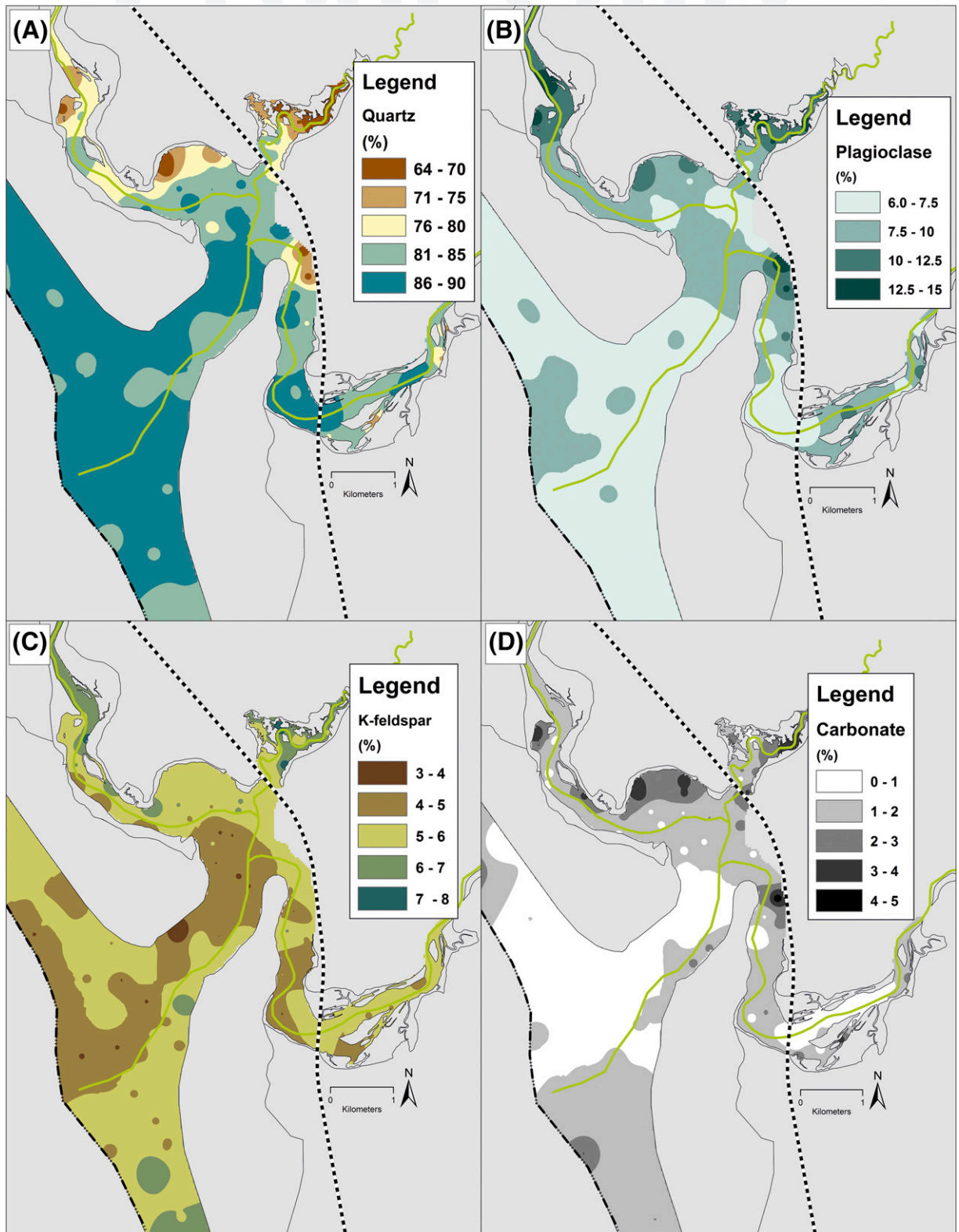
The empirical relationships between composition of sands (QFL; based on sandstone petrology), provenance, and the plate-tectonic setting of the sedimentary basin was first established by Dickinson and Suczek (1979). The “Dickinson model” was later

depositional environments in Figure 13A and B, respectively.

In sediment with grain size finer than upper fine sand (177 μm), illite is typically Fe–Mg rich and relatively well crystalline. In sediment coarser than upper fine sand, illite has a wide range of crystallinity values and compositions (Figure 13A, B). Foreshore sediment is primarily composed of poorly crystalline (illite crystallinity index: >0.25) and relatively Fe–Mg-depleted (Esquevin index: >0.30) illite.

Mineral Abundance: Estuarine Zones and Depositional Environments

Average mineral abundances of the nine depositional environments and eight estuary zones are presented



Q:55 Figure 9. Mapped mineral distribution patterns in the Ravenglass Estuary, United Kingdom. Note that plagioclase and carbonate abundance increase toward the margin of the inner estuary and central basin. Sediment is most quartz rich in outer-estuarine sediment. A slight depletion in K-feldspar is observed in the tidal inlet.

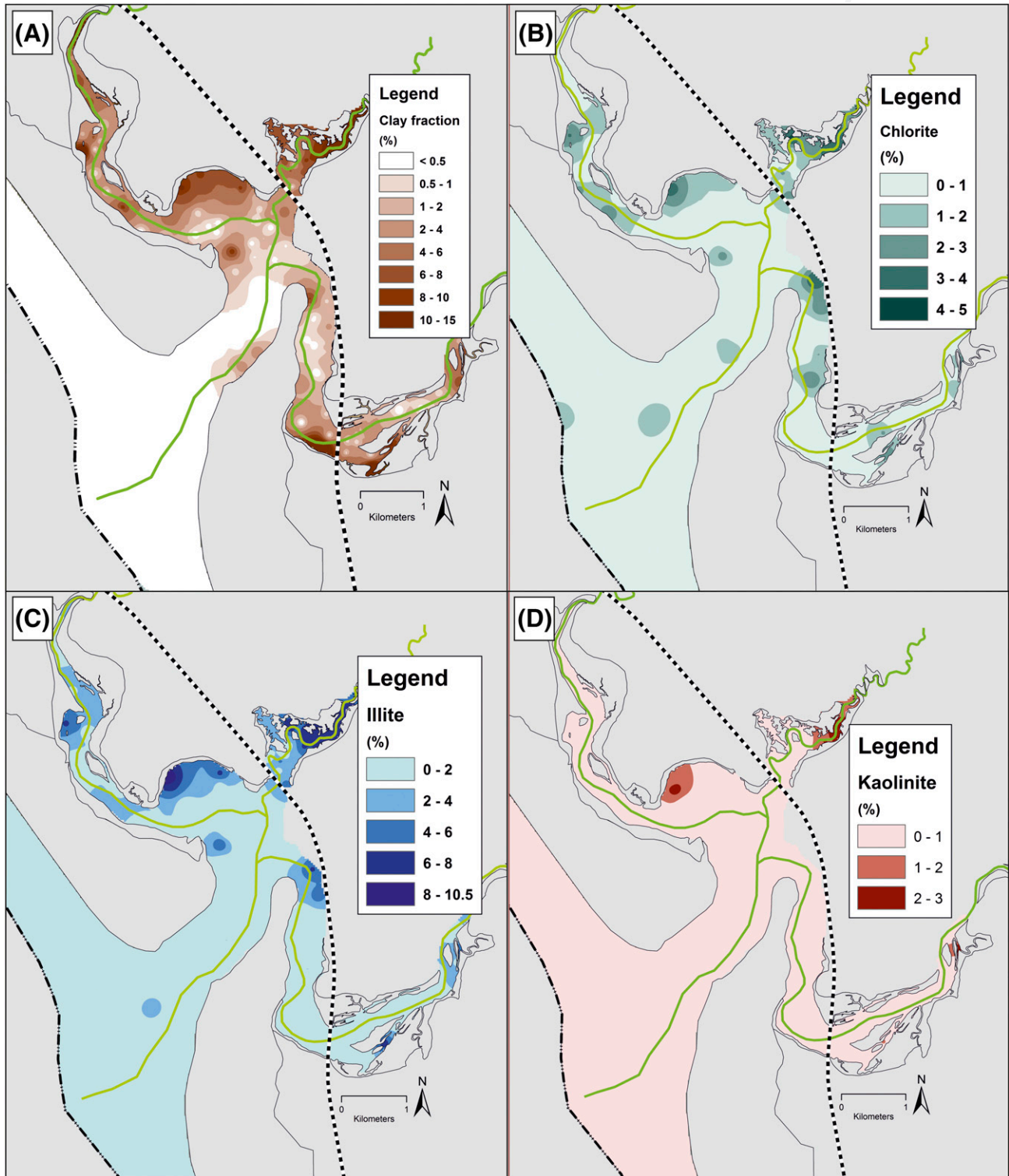


Figure 10. Mapped clay fraction (<2 μm) and clay mineral distribution patterns in the Ravensglass Estuary, United Kingdom. Note that outer-estuarine sediment has a paucity of clay-size material (<0.5%). Illite, chlorite, and kaolinite are most abundant in mud flats and mixed flats; chlorite abundance is elevated in some tidal bar and dune samples (because of a presence of chlorite lithics; see Figures 6A, 12B).

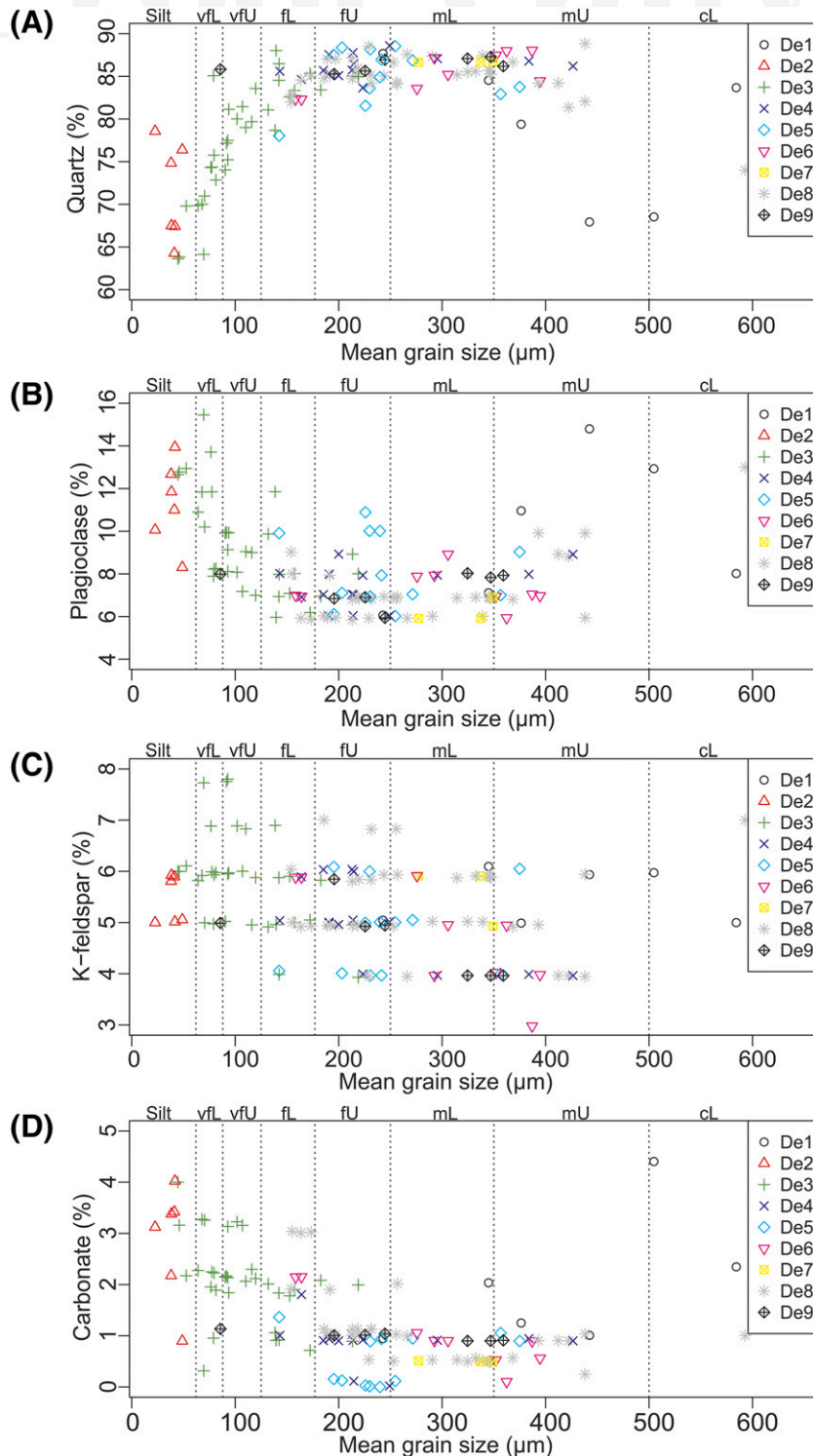


Figure 11. The relationship between specific mineral abundance and mean grain size, colored as a function of depositional environment. Note that quartz abundance increases with an increase in mean grain size, whereas plagioclase and carbonate abundance typically decrease. The K-feldspar abundance slightly decreases with an increase in mean grain size. Depositional environments are labeled accordingly: gravel bed (De1); mud flat (De2); mixed flat (De3); sand flat (De4); tidal bars and dunes (De5); tidal inlet (De6); backshore (De7); foreshore (De8); and proebb delta (De9). Mean grain-size classes are labeled accordingly: silt; lower very fine sand (vfl); upper very fine sand (vfU); lower fine sand (fl); upper fine sand (fU); lower medium sand (mL); upper medium sand (mU); and lower coarse sand (cL).

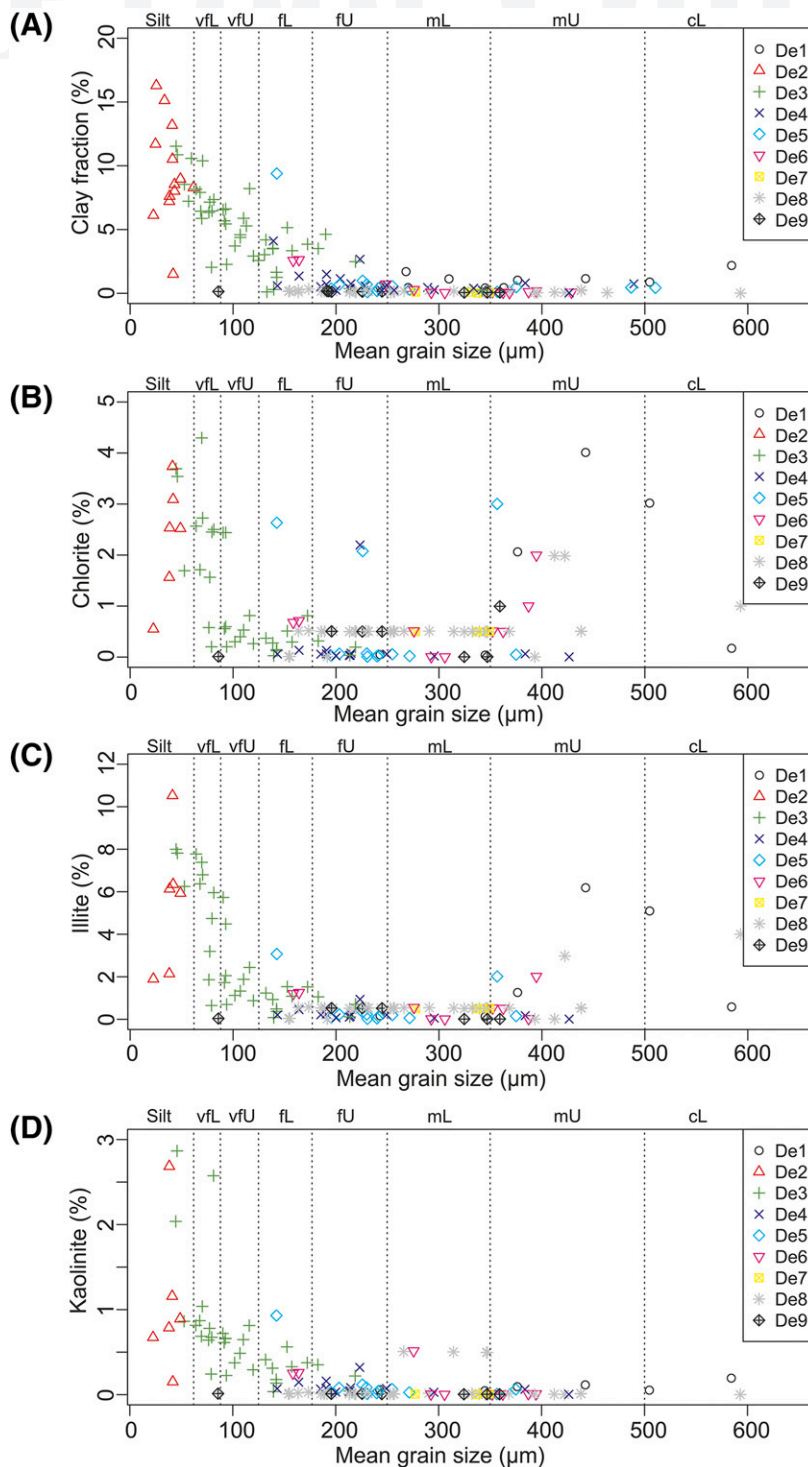


Figure 12. The relationship between clay fraction (<2 μm) and clay mineral abundance with mean grain size, colored as a function of depositional environment. Note that coarser-grained outer-estuarine sediment has a paucity of clay-size material (<0.5%). Illite, chlorite, and kaolinite abundance increase with a decrease in mean grain size (i.e., in mud flats and mixed flats). Chlorite lithics (see Figure 6B) are likely to explain elevated chlorite abundance in tidal dunes and bars despite relatively low clay fraction content. Depositional environments are labeled accordingly: gravel bed (De1); mud flat (De2); mixed flat (De3); sand flat (De4); tidal bars and dunes (De5); tidal inlet (De6); backshore (De7); foreshore (De8); and proebb delta (De9). Mean grain-size classes are labeled accordingly: silt; lower very fine sand (vfl); upper very fine sand (vfU); lower fine sand (fl); upper fine sand (fU); lower medium sand (mL); upper medium sand (mU); and lower coarse sand (cL).

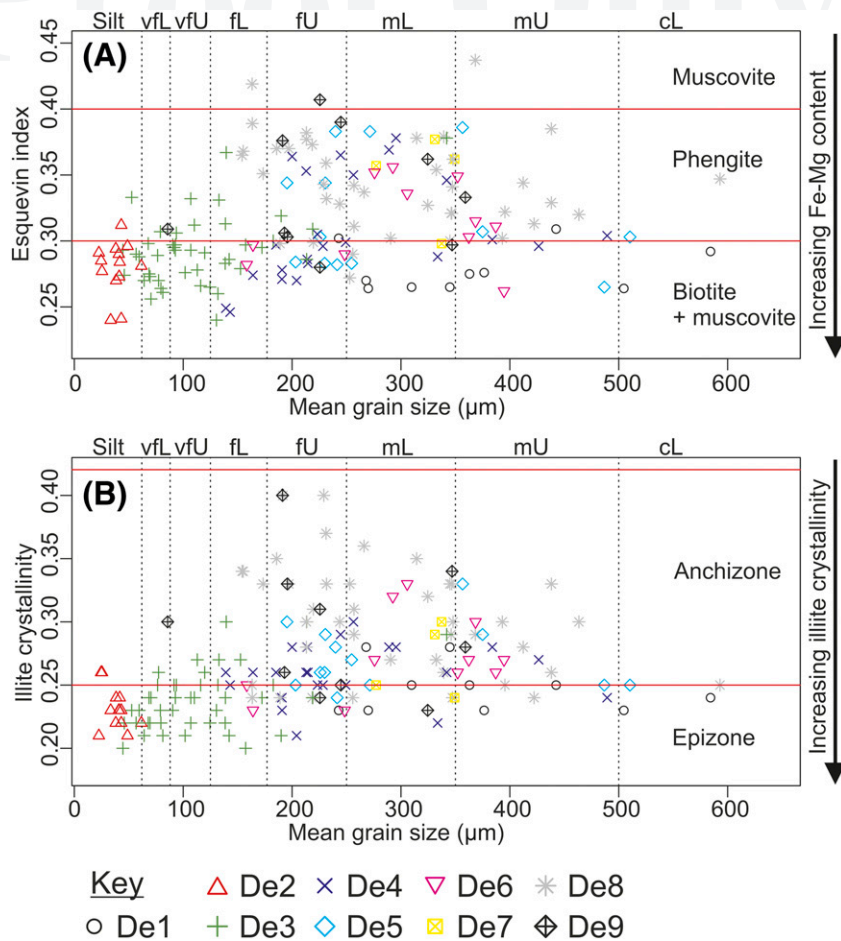


Figure 13. The relationship between (A) illite chemistry (Esquevin index) and (B) illite crystallinity (full width at half maximum of the 10 Å peak) and mean grain size. Note that illite crystallinity and illite Fe–Mg content is reduced with an increase in mean grain size (i.e., in outer-estuarine sediment). Depositional environments are labeled accordingly: gravel bed (De1); mud flat (De2); mixed flat (De3); sand flat (De4); tidal bars and dunes (De5); tidal inlet (De6); backshore (De7); foreshore (De8); and proebb delta (De9). Mean grain-size classes are labeled accordingly: silt; lower very fine sand (vfl); upper very fine sand (vfU); lower fine sand (fl); upper fine sand (fU); lower medium sand (mL); upper medium sand (mU); and lower coarse sand (cL).

revised to improve predictive capabilities using the additive log-ratio transformation by Weltje (2006). Because whole-sediment (QFL-C) mineralogy data, instead of petrographic QFL data, are here reported, it is not possible to follow the methodology outlined by Dickinson and Suczek (1979) or Weltje (2006). However, XRD data, unlike petrographic QFL data, can reveal Esquevin indices (Esquevin, 1969) and illite crystallinity (Kübler, 1964) values that may be used to identify possible sediment source areas and transport pathways (Gingele et al., 2001; Oliveira et al., 2002; Borchers et al., 2011; Bout-Roumazeilles et al., 2013; Du Chatelet et al., 2016).

The sediment composition of the Ravensglass Estuary is arkosic to subarkosic (Figure 7), which is

likely to reflect the drainage of the Eskdale Intrusions and Borrowdale Volcanic Group in the hinterland, in agreement with predictive models produced by Dickinson and Suczek (1979). In the hinterland of the Ravensglass Estuary, there are no carbonate rocks or carbonate-rich drift deposits. As a result, carbonate material is likely to have been primarily derived from gravel beds that have been partly colonized by shell beds in the inner Esk (autochthonous) and derived from offshore (allochthonous). Detrital, chlorite-bearing lithics have been reported to be pyroxene pseudomorphs in the Borrowdale Volcanic Group (Quirke et al., 2015) and the result of chloritization of mafic silicates in the Eskdale Intrusions (Moseley, 1978; Young et al.,

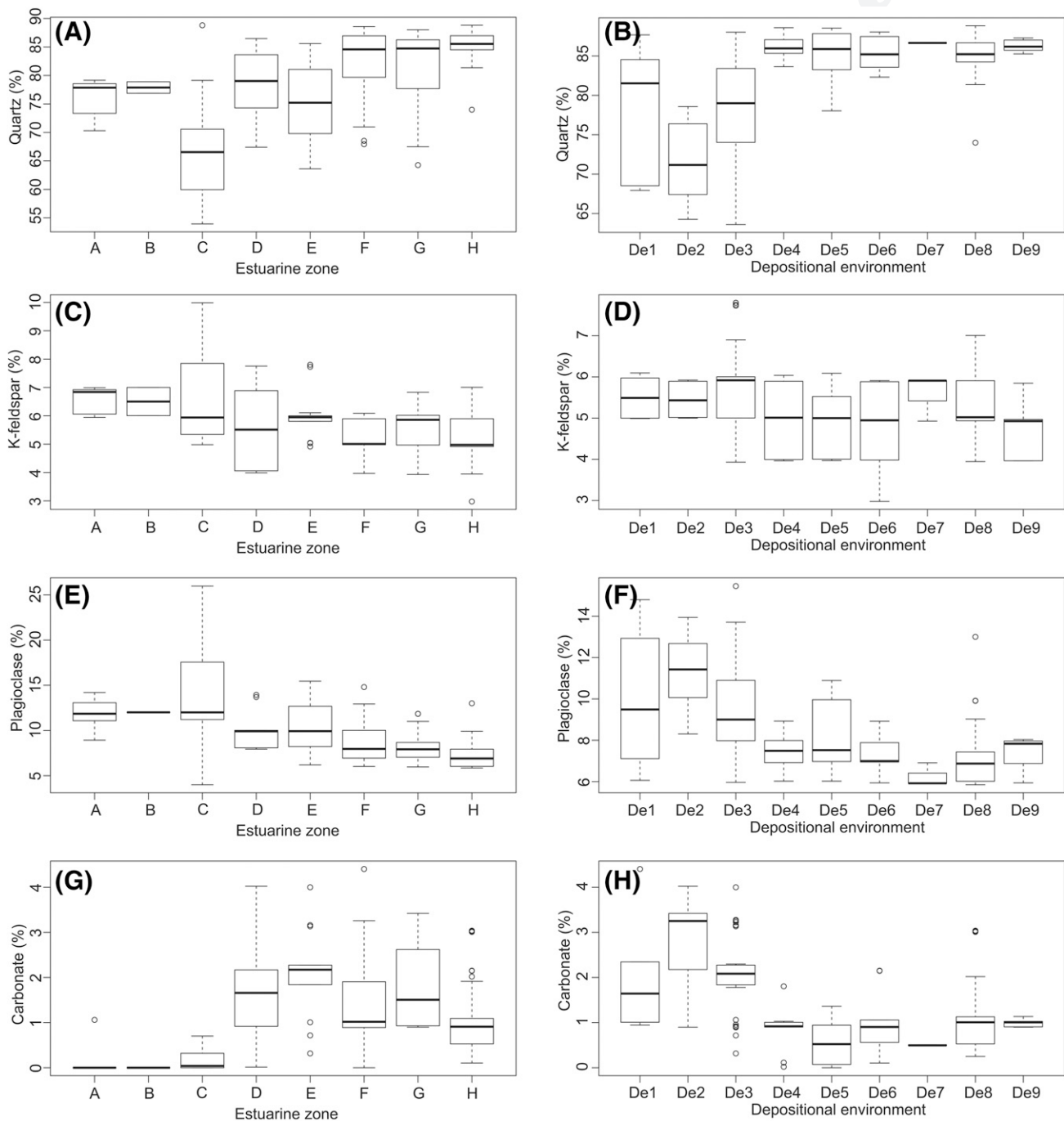


Figure 14. Specific mineral abundance as a function of estuarine zone and depositional environment: (A, B) quartz, (C, D) K-feldspar, (E, F) plagioclase, and (G, H) carbonate. Estuarine zones are labeled accordingly: lower Irt (A); lower Mite (B); lower Esk (C); inner Irt (D); inner Mite (E); inner Esk (F); central basin (G); and outer estuary (H). Depositional environments are labeled accordingly: gravel bed (De1); mud flat (De2); mixed flat (De3); sand flat (De4); tidal bars and dunes (De5); tidal inlet (De6); backshore (De7); foreshore (De8); and proebb delta (De9). Note that outliers (open circles) are defined as an observation that is numerically distant from the rest of the data (i.e., a value that is 1.5 times the interquartile range below the lower quartile and above the upper quartile).

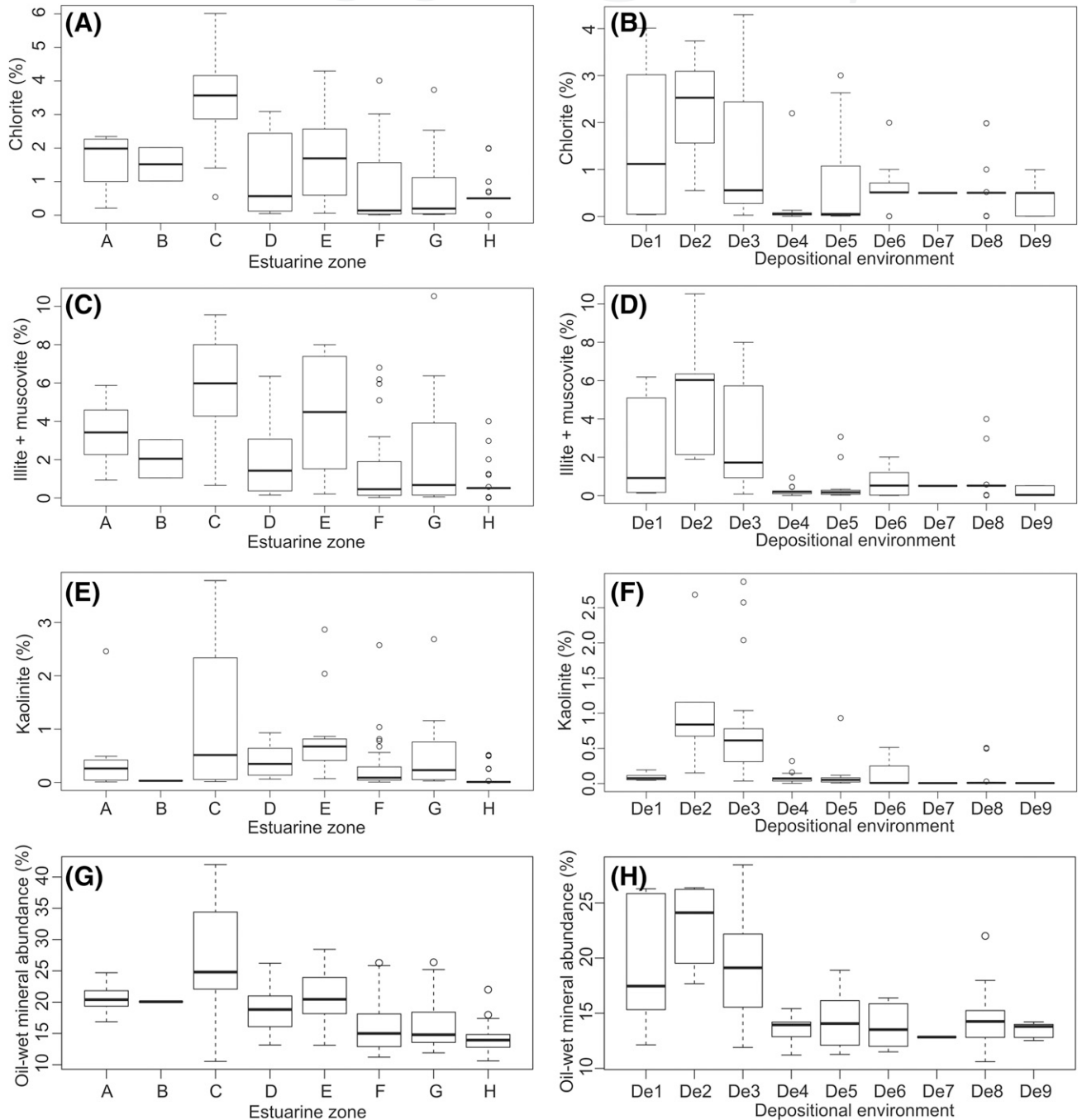





Figure 15. Specific clay mineral abundance and oil-wet mineral abundance as a function of estuarine zone and depositional environment: (A, B) Chlorite, (C, D) illite, (E, F) kaolinite, and (G, H) oil-wet mineral abundance calculated as the sum total of calcite, dolomite, kaolinite (assuming early alteration to kaolinite booklets), hematite, feldspar (assuming weathered; unweathered feldspars are water wet), and Fe-rich chlorite abundance, after Barclay and Worden (2000). Estuarine zones are labeled accordingly: lower Irt (A); lower Mite (B); lower Esk (C); inner Irt (D); inner Mite (E); inner Esk (F); central basin (G); and outer estuary (H). Depositional environments are labeled accordingly: gravel bed (De1); mud flat (De2); mixed flat (De3); sand flat (De4); tidal bars and dunes (De5); tidal inlet (De6); backshore (De7); foreshore (De8); and proebb delta (De9). Note that outliers (open circles) are defined as an observation that is numerically distant from the rest of the data (i.e., a value that is 1.5 times the interquartile range below the lower quartile and above the upper quartile).

Table 3. Post Hoc Tukey's Honestly Significant Difference Test (Following Analysis of Variance) Results Are Presented Here as a Correlation Matrix Comparing Quartz, K-Feldspar, Plagioclase, and Carbonate Abundance Data between the Various Depositional Environments from Ravenglass Estuary

		Depositional Environment							
		De1	De2	De3	De4	De5	De6	De7	De8
Q:63	Quartz								
	De2	-7.13	X 						
	De3	-0.84	6.28+						
	De4	7.5*	14.66***	8.37***					
	De5	6.47	13.59***	7.31***	-1.05	X			
	De6	6.78	13.90***	7.62***	-0.75	0.30	X		
	De7	8.04	15.16***	8.88***	0.51	1.56	1.26	X	
	De8	6.42*	13.54***	7.26*	-1.11	-0.06	-0.36	-1.62	X
	De9	7.69+	14.8***	8.53***	0.16	1.22	0.92	-0.34	1.28
	K-feldspar	De2	-0.06	X					
De3		0.33	0.39	X					
De4		-0.51	-0.45	-0.84+	X				
De5		-0.66	-0.60	-0.99*	-0.15	X			
De6		-0.78	-0.72	-1.11*	-0.27	-0.12	X		
De7		0.08	0.13	-0.26	0.59	0.73	0.86	X	
De8		-0.13	-0.07	-0.46	0.38	0.53	0.65	-0.21	X
De9		-0.85	-0.79	-1.18*	-0.34	-0.19	-0.07	-0.93	-0.72
Plagioclase		De2	1.33	X					
	De3	-0.53	-1.86	X					
	De4	-2.56	-3.89***	-2.03**	X				
	De5	-1.81	-3.14*	-1.28	0.75	X			
	De6	-2.69	-4.09**	-2.16*	-0.13	-0.88	X		
	De7	-3.73	-5.06**	-3.2+	-1.17	-1.92	-1.04	X	
	De8	-2.79	-4.11***	-2.26***	-0.23	-0.98	-0.10	0.94	X
	De9	-2.63	-3.95**	-2.09	-0.06	-0.81	0.07	1.11	0.16
	Carbonate	De2	0.84	X					
De3		0.07	-0.77	X					
De4		-1.12	-1.96***	-1.18***	X				
De5		-1.45**	-2.29***	-1.52***	-0.34	X			
De6		-0.97	-1.81***	-1.03***	0.15	0.48	X		
De7		-1.50	-2.34***	-1.56*	-0.38	-0.04	-0.53	X	
De8		-0.92	-1.75***	-0.98***	0.20	0.54	0.05	0.58	X
De9		-1.01	-1.85***	-1.08*	0.11	0.44	-0.04	0.49	-0.10

Bold values indicate paired zones, or depositional environments are statistically different. Levels of statistical significance (*p* value) are coded as follows: marginally significant (+) when the *p* value is <0.1; significant (*) when the *p* value is <0.05; very significant (**) when the *p* value is <0.01; and extremely significant (***) when the *p* value is <0.001. Nonbolded values represent no significant difference when the *p* value is >0.1. Depositional environments are labeled accordingly: gravel bed (De1); mud flat (De2); mixed flat (De3); sand flat (De4); tidal bars and dunes (De5); tidal inlet (De6); backshore (De7); foreshore (De8); and proebb delta (De9).

Table 4. Post Hoc Tukey's Honestly Significant Difference Test (Following Analysis of Variance) Results Are Presented Here as a Correlation Matrix Comparing Quartz, K-Feldspar, Plagioclase, and Carbonate Abundance Data between the Various Estuarine Zones from Ravenglass Estuary

	Estuarine Zone						
	A	B	C	D	E	F	G
Quartz							
B	1.9	X					
C	-8.4*	-10.3	X				
D	2.9	0.9	11.2***	X			
E	-1.5	-3.4	6.8	-4.4	X		
F	6.6*	4.7	14.9***	3.7	8.1***	X	
G	5.1	3.2	13.5***	2.3	6.7*	-1.4	X
H	9.4***	7.5	17.8***	6.52*	10.9***	2.8	4.3
K-feldspar							
B	0.0	X					
C	0.3	0.4	X				
D	-1.0	-0.9	-1.3+	X			
E	-0.5	-0.5	-0.9	0.4	X		
F	-1.3**	-1.3	-1.7***	-0.4	-0.8	X	
G	-1.1+	-1.1	-1.5**	-0.2	-0.6	0.2	X
H	-1.36**	-1.3	-1.7***	-0.4	-0.8+	0.0	-0.2
Plagioclase							
B	0.1	X					
C	2.6	2.6	X				
D	-1.9	-2.0	-4.5**	X			
E	-1.4	-1.5	-4.0**	0.5	X		
F	-3.5**	-3.6	-6.2***	-1.6	-2.1	X	
G	-3.7**	-3.8	-6.4***	-1.8	-2.3	-0.2	X
H	-4.7***	-4.8	-7.4***	-2.8*	-3.3	-1.2	-1.0
Carbonate							
B	-0.1	X					
C	0.1	0.2	X				
D	1.6***	1.8	1.5**	X			
E	1.8***	2.1*	1.9***	0.3	X		
F	1.2**	1.3	1.1*	-0.4	-0.7	X	
G	1.7***	1.8+	1.6***	0.0	-0.3	0.5	X
H	0.9+	1.0	0.8	-0.7	-1.1**	-0.3	-0.8*

Bold values indicate paired zones, or depositional environments are statistically different. Levels of statistical significance (*p* value) are coded as follows: marginally significant (+) when the *p* value is <0.1; significant (*) when the *p* value is <0.05; very significant (**) when the *p* value is <0.01; and extremely significant (***) when the *p* value is <0.001. Nonbolded values represent no significant difference when the *p* value is >0.1. Estuarine zones are labeled accordingly: lower lrt (A); lower Mite (B); lower Esk (C); inner lrt (D); inner Mite (E); inner Esk (F); central basin (G); and outer estuary (H).

1986; Quirke et al., 2015). As a result, chlorite-bearing lithics in the Ravenglass Estuary (Figure 6A) are likely to have been sourced from the Borrowdale Volcanic Group and chloritized areas of the Eskdale Intrusions, both of which have been reworked and incorporated into overlying Quaternary drift deposits (Merritt and Auton, 2000).

Illite that is Fe-Mg rich and relatively well crystalline (Figure 13), which dominates sediment that is finer than upper fine sand (<177 μm), is likely sourced from the Ravenglass Till Member because such values are typical of physically eroded, unweathered rocks (and therefore till; Chamley, 1989). In contrast, sediment that is coarser than upper fine sand (>177 μm)

Table 5. Post Hoc Tukey's Honestly Significant Difference Test (Following Analysis of Variance) Results Are Presented Here as a Correlation Matrix Comparing Chlorite, Illite, and Kaolinite Abundance Data between the Various Depositional Environments from Ravenglass Estuary

	Depositional Environment							
	De1	De2	De3	De4	De5	De6	De7	De8
Chlorite								
De2	0.77	X						
De3	-0.37	-1.15	X					
De4	-1.35+	-2.12***	-0.98**	X				
De5	-0.89	-1.66*	-0.52	0.46	X			
De6	-0.90	-1.67*	-0.53	0.45	-0.01	X		
De7	-1.06	-1.83	-0.69	0.29	-0.17	-0.16	X	
De8	-1.01	-1.79***	-0.64+	0.33	-0.13	-0.11	0.05	X
De9	-1.20	-1.97**	-0.83	0.15	-0.31	-0.30	-0.14	-0.18
Illite								
De2	3.26*	X						
De3	0.74	-2.52*	X					
De4	-1.99	-5.24***	-2.73***	X				
De5	-1.69	-4.95***	-2.43**	0.30	X			
De6	-1.56	-4.82***	-2.30*	0.43	0.13	X		
De7	-1.73	-4.99**	-2.47**	0.26	-0.04	-0.17	X	
De8	-1.62	-4.88***	-2.36***	0.37	0.07	-0.06	0.11	X
De9	-2.00	-5.26***	-2.74***	-0.02	-0.31	-0.45	-0.27	-0.38
Kaolinite								
De2	0.96***	X						
De3	0.59**	-0.37	X					
De4	-0.01	-0.97***	-0.59***	X				
De5	0.03	-0.93***	-0.56***	0.04	X			
De6	0.03	-0.94***	-0.56***	0.03	0.00	X		
De7	-0.09	-1.05***	-0.68+	-0.08	-0.12	-0.11	X	
De8	-0.03	-0.99***	-0.61***	-0.02	-0.06	-0.05	0.06	X
De9	-0.09	-1.05***	-0.68**	-0.08	-0.12	-0.11	0.00	-0.06

Bold values indicate paired zones, or depositional environments are statistically different. Levels of statistical significance (*p* value) are coded as follows: marginally significant (+) when the *p* value is <0.1; significant (*) when the *p* value is <0.05; very significant (**) when the *p* value is <0.01; and extremely significant (***) when the *p* value is <0.001. Nonbolded values represent no significant difference when the *p* value is >0.1. Depositional environments are labeled accordingly: gravel bed (De1); mud flat (De2); mixed flat (De3); sand flat (De4); tidal bars and dunes (De5); tidal inlet (De6); backshore (De7); foreshore (De8); and proebb delta (De9).

contains illite that has a wide range of crystallinity values and compositions (Figures 13A, B); this is characteristic of both chemically weathered rocks that have lost divalent cations (Fe and Mg) and physically eroded, unweathered rocks (Chamley, 1989).

Results of XRD show that rigid framework grains (e.g., quartz) and brittle minerals (e.g., feldspar) are present in high abundance in both the clay and silt fraction of drift deposits; this is probably caused by extensive subglacial comminution. The relatively high concentration of quartz in the clay and silt fraction of Ravenglass Estuary sediment is probably in

contrast to other nonglaciated sedimentary basins that are typically depleted in quartz in the finest sediments (Odom et al., 1976). Furthermore, the Ravenglass Till Member may also be an important source of plagioclase, with abundances of up to 14%.

Controls on Mineral Distribution Patterns

Provenance Controls and Sediment Transport Pathways
Provenance studies (based on sandstone composition) may be undertaken to unravel and characterize the complex history that has led to the production and

Table 6. Post Hoc Tukey's Honestly Significant Difference Test (Following Analysis of Variance) Results Are Presented Here as a Correlation Matrix Comparing Chlorite, Illite, and Kaolinite Abundance Data between the Various Estuarine Zones from Ravenglass Estuary

	Estuarine Zone						
	A	B	C	D	E	F	G
Chlorite							
B	0.01	X					
C	1.92**	1.91	X				
D	-0.30	-0.31	-2.22***	X			
E	0.36	0.35	-1.56**	0.66	X		
F	-0.69	-0.70	-2.61***	-0.39	-1.05*	X	
G	-0.73	-0.74	-2.65***	-0.43	-1.09+	-0.04	X
H	-0.98	-0.99	-2.89***	-0.68	-1.34***	-0.29	-0.25
Illite							
B	-1.41	X					
C	2.49	3.90	X				
D	-1.30	0.11	-3.79**	X			
E	0.72	2.13	-1.77	2.02	X		
F	-2.04	-0.63	-4.53***	-0.74	-2.76**	X	
G	-1.24	0.17	-3.72***	0.06	-1.96	0.80	X
H	-2.89**	-1.48	-5.38***	-1.59	-3.61***	-0.85	-1.65+
Kaolinite							
B	-0.43	X					
C	0.89*	1.31+	X				
D	-0.06	0.37	-0.95*	X			
E	0.39	0.83	-0.49	0.45	X		
F	-0.17	0.26	-1.06***	-0.11	-0.56+	X	
G	0.03	0.46	-0.86*	0.09	-0.36	0.20	X
H	-0.40	0.03	-1.29***	-0.34	-0.79***	-0.23	-0.43

Bold values indicate paired zones, or depositional environments are statistically different. Levels of statistical significance (*p* value) are coded as follows: marginally significant (+) when the *p* value is <0.1; significant (*) when the *p* value is <0.05; very significant (**) when the *p* value is <0.01; and extremely significant (***) when the *p* value is <0.001. Nonbolded values represent no significant difference when the *p* value is >0.1. Estuarine zones are labeled accordingly: lower Irt (A); lower Mite (B); lower Esk (C); inner Irt (D); inner Mite (E); inner Esk (F); central basin (G); and outer estuary (H).

the evolution of sediments, from initial weathering and erosion in the source sediment area and passing through to sediment transport and temporary storage and finally burial and lithification (Caracciolo et al., 2012). For example, the vertical (stratified) differences in plagioclase content were reported to reflect differences in sediment provenance in the Statfjord Formation, Gullfaks field (Dalland et al., 1995).

It is noteworthy that grain-size dependence of sediment composition may lead to bias in provenance studies (Garzanti et al., 2009). However, despite River Irt and Mite (northern drainage basin) sediment having a comparable mean grain size (Figure 5A), River Esk sediment (southern drainage basin) is relatively chlorite and feldspar rich (Figure 15A). The

enrichment of feldspar and chlorite may reflect the drainage of chloritic and feldspathic Eskdale Intrusions, which is primarily restricted to the River Esk drainage basin (south of Muncaster Fell; Figure 1). An important outcome of this study is that, despite the Rivers Irt and Esk having different fluvial sediment compositions, counterpart inner-estuarine zones (inner Irt, zone D; inner Esk, zone F) show no statistical difference in composition (Tables 3–6). Thus, provenance signals have been removed, presumably because of intense estuarine mixing (likely caused by the macrotidal regime and short estuarine length) and possible dilution by a second estuarine mineral assemblage (e.g., internal erosion of glacial deposits throughout the estuary).

Hydrodynamic Controls, Mechanical Breakdown, and Physical Sorting of Minerals by Grain Size

The findings of Odom et al. (1976) are commonly invoked to explain mineral distribution patterns in many sandstone reservoirs. Odom et al. (1976) reported that feldspar abundance and distribution in a range of sandstones was controlled by the degree of sediment abrasion (grain size), transport processes, and depositional environment. Results presented by Odom et al. (1976) show that feldspar tends to be concentrated in the fraction of the sediment less than 125 μm (upper very fine sand) or, in some cases, the coarse silt fraction. Field and Pilkey (1969) showed that feldspar in shelf and beach sands is concentrated in the fine and very fine sand fractions as a result of intense abrasion. In agreement with results from Odom et al. (1976), plagioclase abundance in Ravenglass sediment significantly decreases in abundance above a critical grain-size threshold of 125 μm . Odom et al. (1976) hypothesized that 125 μm represents a threshold below which feldspar tends to be less susceptible to further size reduction by abrasion. However, results of this study show that plagioclase is susceptible to reduction less than 125 μm , most likely caused by extensive subglacial comminution (Figure 11). Consequently, plagioclase typically continues to increase in abundance with a reduction in mean grain size between the grain-size classes silt to upper very fine sand (62–125 μm). Glacial comminution has previously been shown to lead to both quartz and feldspar being concentrated in clay and silt fractions (Stevens, 1991). In contrast, K-feldspar appears to show little relationship with mean grain size and displays only a minor depletion in sediment upon the northern foreshore, where the sediment is typically coarser than upper fine sand (>250 μm). The depletion in K-feldspar and carbonate in northern foreshore sediment may reflect the dominant wave direction originating from the southwest.

Quartz, a rigid-framework grain, is relatively resistant to sediment abrasion and grain-size reduction in comparison with brittle-framework grains such as feldspars, carbonate, and clay minerals. Estuarine hydrodynamics cause the physical sorting of grains by size and consequently have led to a relatively uniform high abundance (~85%) of quartz in depositional environments composed of relatively coarse sediment (>177–350 μm). Depositional environments with a mean grain size between 62 and 177 μm typically

show a progressive increase in quartz abundance with an increase in mean grain size.

Allochthonous (derived from offshore) carbonate material has likely suffered extensive abrasion caused by repeated wave action prior to being transported and deposited into the estuarine system. Equally, autochthonous carbonate (from gravel beds that are partly colonized by shell beds in the inner Esk) has likely experienced extensive reworking and abrasion by strong tidal currents. Consequently, carbonate (>95% calcite) material is most abundant in low-energy depositional environments, in sediment that has a mean grain size less than upper fine sand (177 μm) (Figure 11D). In contrast, in sediment that has a grain size greater than upper fine sand (177 μm), carbonate material will end to be resuspended during marine inundation caused by tidal currents and wave action.

Chlorite, illite, and kaolinite, as expected, dominate the clay fraction of estuarine sediment and therefore have the greatest absolute abundance in relatively low-energy depositional environments (mud flats and mixed flats). However, relatively high-energy tidal dune, tidal bar, foreshore, and tidal inlet depositional environments locally contain elevated chlorite concentrations (Figure 12B). The enrichment in chlorite cannot be explained by an increase in clay-size material (Figure 12A) and instead probably reflects the accumulation of chlorite lithics (Figure 6A).

Early Mineral Alteration and Chemical Breakdown Controls

At the fluvial-marine interface, there is a merging of terrigenous sediment transported by low-salinity, relatively organic- and iron-rich continental waters with high-salinity marine conditions, which have high aqueous sulfate concentration and a locally high oxidation state (Boyle et al., 1974, 1977; Sholkovitz, 1978; Sholkovitz et al., 1978; Berner and Berner, 2012). Consequently, early mineral alteration is significant in marginal marine settings and remains a potential control on mineral distribution patterns in the Ravenglass Estuary. Based on high-resolution QEMSCAN (SEM-EDS imaging), Daneshvar and Worden (2018) reported that detrital K-feldspar grains are preferentially rimmed by neofomed illite, whereas plagioclase grains may be preferentially rimmed by neofomed kaolinite in the Ravenglass Estuary; this was suggested to be evidence for continued

mineral alteration of the estuarine sediment. The concept of early mineral alteration in the Ravenglass Estuary remains possible; however, it should be noted that intense alteration of feldspars in the hinterland of the Ravenglass Estuary has been widely reported (Moseley, 1978; Young et al., 1986; Quirke et al., 2015). As a result, it is not impossible that kaolinized plagioclase and illitized K-feldspars may be an inherited feature of the sediment and not caused by continued weathering in the estuary.

SIGNIFICANCE: FACILITATING SANDSTONE RESERVOIR QUALITY PREDICTION DURING PETROLEUM EXPLORATION, APPRAISAL, AND FIELD DEVELOPMENT AND PRODUCTION

The economic viability of sandstone reservoirs can be assessed by prediction of (1) porosity, which controls petroleum in-place volumes, and (2) permeability, which controls the rate at which petroleum can be produced (Worden et al., 2018). Sandstone texture (e.g., grain size, grain-size sorting, and matrix content) and composition are major controls on the porosity, permeability, and wettability state of sandstone reservoirs (Beard and Weyl, 1973; Scherer, 1987a, b; Bloch, 1991; Ramm and Bjorlykke, 1994; Barclay and Worden, 2000). This study can be used by analogy to better predict compositional and textural variation in ancient and deeply buried estuarine sandstones, with knowledge of how primary depositional texture and mineralogy may alter during burial diagenesis.

Compositional and Textural Variation in the Ravenglass Estuary, United Kingdom: Implications for Reservoir Quality and Provenance Signals in Estuarine Sandstones

The proportion of framework grain types is widely reported to significantly impact the diagenetic evolution and reservoir quality of sandstones (Morad et al., 2010). For example, feldspar and plutonic rock fragment dissolution may lead to the formation of intergranular and moldic pores during eo- and mesodiagenesis, creating secondary porosity and enhancing reservoir quality (Morad et al., 2010). As a result, based upon the hinterland geology, sedimentary provenance

models enable broadly accurate predictions of sandstone composition during hydrocarbon exploration, field appraisal, and development (Dickinson and Suczek, 1979; Weltje, 2006; Garzanti et al., 2009). For example, the Dickinson model (Dickinson and Suczek, 1979) may be used during hydrocarbon exploration to make general predictions on sediment composition; however, it does not lend itself easily to other applications, such as regional studies of multisource basin fills (Weltje, 2006). In addition, petrographic QFL studies may fail to distinguish between glacial and nonglacial derived sediments, unlike XRD provenance studies that reveal Esquevin indices, which have proven to be a provenance indicator in the Ravenglass Estuary (Figure 13). However, it is possible that Esquevin index and illite crystallinity data sets may not be appropriate when studying sandstones that may have commenced illite alteration during burial.

Results of this study have shown that fluvial sediments in the Rivers Irt, Mite, and Esk broadly reflect the drainage of different bedrocks, soil types, and drift deposits and therefore have different sediment compositions (Figure 7). For example, River Esk sediment is relatively feldspathic and chlorite enriched (Figures 14, 15). However, the proportions of minerals in sediment in the counterpart inner-estuarine zones (i.e., inner Esk and inner Irt) are relatively uniform (Tables 4, 6). The dilution of provenance signals in Ravenglass inner-estuarine zones is most likely caused by intense mixing promoted by strong tidal currents and a short estuarine length. Consequently, reservoir quality studies of mixed-energy turbulent estuarine sandstones may benefit from removing provenance signals from inner-estuarine zones and instead focus on modeling the redistribution of specific minerals based on likely estuarine hydrodynamics and typical subsequent diagenetic pathways.

Compositional and Textural Variation in the Ravenglass Estuary, United Kingdom: Implications for the Diagenetic Alteration and Reservoir Quality of Estuarine Sandstones

Several studies, such as Morad et al. (2010) and Worden and Morad (2003), have shown that there is a finite number of common processes that may lead to

the alteration of primary depositional mineralogy and texture during burial diagenesis. In this section, results from the Ravenglass Estuary have been used to predict the distribution of sandstone reservoir quality in ancient and deeply buried estuarine sandstone reservoirs in the eodiagenetic (<2000 m [<6562 ft]; $<60^{\circ}\text{C}$ – 70°C) and mesodiagenetic (>2000 m [>6562 ft]; $>60^{\circ}\text{C}$ – 70°C) realms (Figure 16).

Eodiagenesis: Impact on Estuarine Sandstone Reservoir Quality

During eodiagenesis, an abundance of ductile grains will promote mechanical compaction and pseudo-matrix formation (Scherer, 1987a, b; Bloch, 1991; Ramm and Bjorlykke, 1994; Worden et al., 2000; Morad et al., 2010). As a result, relatively low primary porosity values associated with poorly sorted and fine-grained sediment (Beard and Weyl, 1973), such as mud- and mixed-flat sediments, are likely to experience rapid loss of porosity and permeability during eodiagenesis because of an abundance of ductile grains (Figure 16A–D).

Meteoric water flushing, which can lead to the dissolution and kaolinization of reactive silicate minerals (primarily feldspars) (Glasmann et al., 1989), is particularly common in estuaries (especially at the head of the estuary, away from marine influence) because marginal marine systems are highly sensitive to relative sea-level changes (Ketzer et al., 2003; Worden and Burley, 2003; Morad et al., 2010, 2012). Because mud flats, mixed flats, and River Esk sediments contain an abundance of feldspars and a rich stew of reactive silicate minerals, they are likely to contain enhanced secondary porosity; authigenic kaolinite booklets may, however, occlude porosity (Figure 16).

The K-feldspar overgrowths may occlude porosity and diminish permeability; however, they typically form in such low quantities they rarely impact reservoir quality (Morad et al., 2010), and K-feldspar abundance is relatively evenly distributed in the Ravenglass Estuary.

Large volumes of early carbonate cement can obliterate porosity and have commonly been observed in foreshore and backshore sandstones, leading to the term beachrock (Kantorowicz et al., 1987). However, porosity may be enhanced because of the

subsequent formation of intragranular and moldic pores through the dissolution of carbonate grains; this is most likely to occur in carbonate-enriched mud flats and mixed flats (Figure 16). Furthermore, early carbonate cement may increase the mechanical strength of sediments (Morris et al., 2006) and may therefore preserve remaining porosity during subsequent compaction. As a result, better reservoir quality may be found in estuarine depositional environments that initially contained a small, but as yet undefined (“Goldilocks” scenario), amount of carbonate material.

In the Ravenglass Estuary, biofilm-mediated detrital clay coats are most extensive in mud flats and mixed flats, with only partial coatings present on sand grains in sand flats, tidal bars, and dunes; detrital clay coats are almost entirely absent in outer-estuarine sediment (Wooldridge et al., 2017a, b, 2018). Detrital clay coat development in the primary depositional environment and via eodiagenetic processes, (e.g., infiltration [Matlack et al., 1989]), are important because porosity-preserving authigenic clay coats are reported to form through the thermally driven recrystallization of detrital clay coats (Ehrenberg, 1993) as well as through the in situ growth from the authigenic alteration of detrital precursors and eodiagenetic phases (Hillier, 1994; Aagaard et al., 2000; Worden and Morad, 2003; Ajdukiewicz and Larese, 2012). The impact of detrital and authigenic clay coats is further discussed in the subsequent section.

Mesodiagenesis: Impact on Estuarine Sandstone Reservoir Quality

During mesodiagenesis, one of the major controls on reservoir quality is the transition from quartz being relatively inert and relatively unreactive to becoming more soluble as a result of increased effective stress and burial temperatures in excess of 80°C – 100°C (Worden and Burley, 2003; Worden et al., 2018).

Quartz cementation is likely to be most extensive in mud flats and mixed flats that host an abundance of micas and illite, which promote quartz cementation and pressure dissolution at grain contacts (Oelkers et al., 1996; Meyer et al., 2006; Trewin and Fallick, 2009), as well as quartz-rich depositional environments (Walderhaug, 1994a, b), such as outer-estuarine sediments.

In contrast, chlorite and mixed illite/chlorite clay coats may preserve porosity through the inhibition of

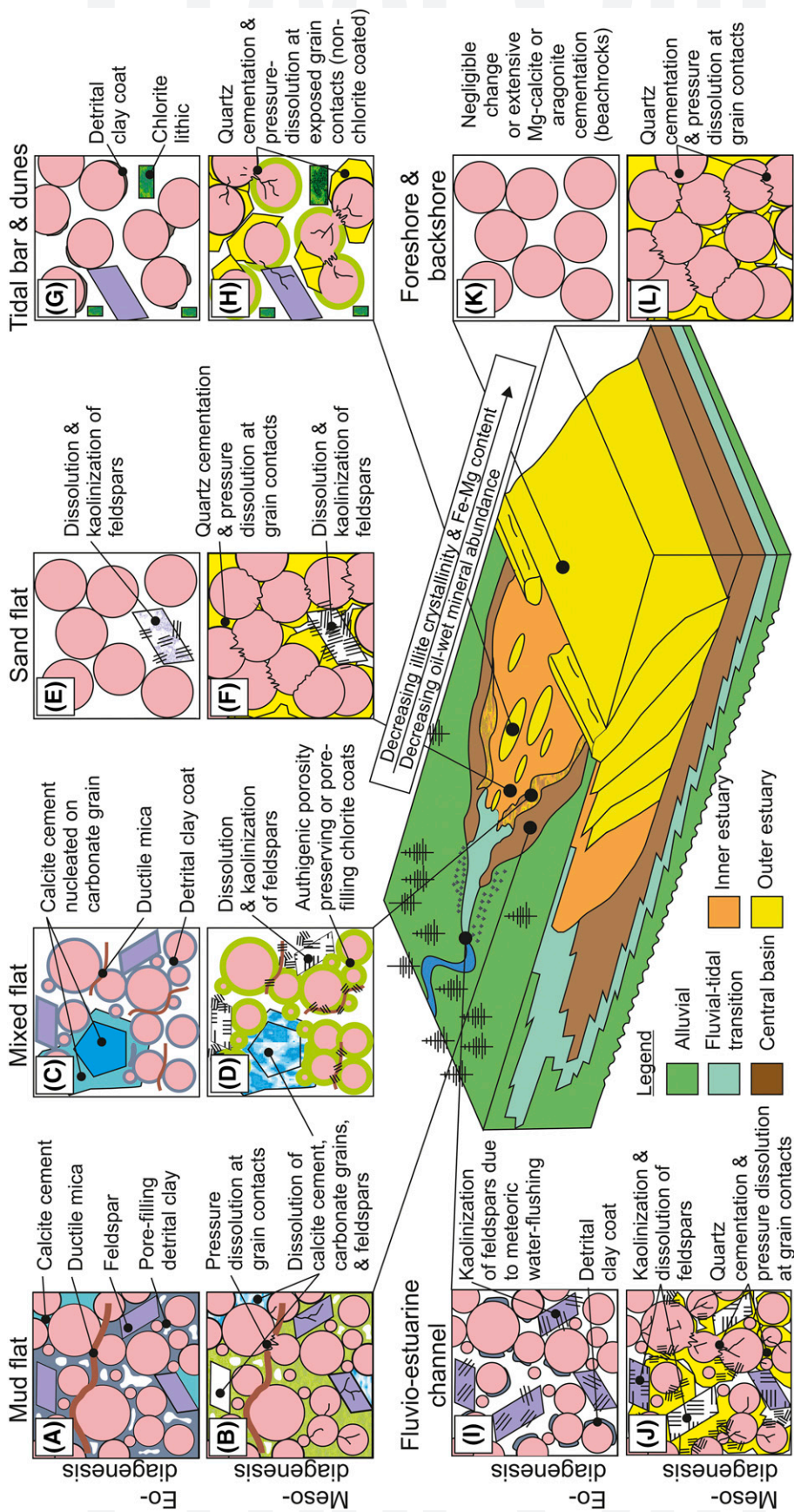


Figure 16. Summary schematic to facilitate reservoir quality prediction based upon compositional variation in the wave- and tide-dominated Ravenglass Estuary, United Kingdom and likely eo- and mesodiagenetic pathways, after Worden and Morad (2003) and Morad et al. (2010). Oil-wet mineral abundance is the sum total of calcite, dolomite, kaolinite (assuming early alteration to kaolinite booklets), hematite, feldspar (assuming weathered; unweathered feldspars are water wet), and Fe-rich chlorite abundance, after Barclay and Worden (2000). Detrital clay coat coverage (precursor to authigenic clay coats during mesodiagenesis) is based on previous studies in the Ravenglass Estuary (Woodruff et al., 2017a, b, 2018). For each depositional environment, a schematic petrographic image (A–L) under eodiagenetic (<2000 m [<6562 ft]; <60°C–70°C) and mesodiagenetic (>2000 m [>6562 ft]; >60°C/70°C) conditions (above and below, respectively), is shown. The subsurface part of the block diagram is modified from Dairymple et al. (1992).

quartz cementation (Ehrenberg, 1993; Dowey et al., 2012; Stricker et al., 2016; Stricker and Jones, 2018). Therefore, the reservoir quality of the Ravenglass Estuary, if it was to be buried to temperatures exceeding 80°C–100°C, would largely depend on whether detrital clay coats (Wooldridge et al., 2017a, b, 2018) formed chlorite clay coats and enhanced reservoir quality or formed illite clay coats and promoted quartz cementation and pressure dissolution. Chlorite clay coats are most likely to form in inner-estuarine tidal bars and dunes because of an enrichment of detrital chlorite (Figure 12C) and sufficient clay content to form clay coats, reported to be as little as 1%–2% of the rock volume by Bloch et al. (2002).

In the Ravenglass Estuary, plagioclase is most abundant in fluvial and mud- and mixed-flat sediments (Figures 11C, 14E). As a result, by analogy, plagioclase albitization, which may provide small amounts of carbonate and clay mineral cements (Morad et al., 2010), is likely to be most extensive in fluvial and tidal flat sandstones. In contrast, K-feldspar is relatively evenly distributed throughout the Ravenglass Estuary, and therefore, any diagenetic processes requiring K-feldspar are not likely to be facies dependent.

Enhanced secondary porosity caused by the dissolution of detrital carbonate grains and eodiagenetic calcite cement is likely to be most significant in carbonate-rich depositional environments (i.e., tidal flats; Figure 11D).

Compositional Variation in the Ravenglass Estuary, United Kingdom: Implications for Reservoir Wettability

Wettability is defined as the tendency of a fluid, in the presence of another (immiscible) fluid, to spread along a solid surface (Crocker and Marchin, 1988). Whether a reservoir rock is primarily water wet (water bound to the surface of grains) or oil wet (oil bound to the surface of grains) may have significant implication from economic viability (e.g., petroleum in-place and diagenetic processes, such as the extent of quartz cementation [Barclay and Worden, 2000]). Controls on wettability in sandstone reservoirs include petroleum composition, reservoir mineralogy, pressure, and temperature (Barclay and Worden, 2000). As a result, compositional variations in the

Ravenglass Estuary may be used, by analogy, to facilitate the prediction of the spatial distribution and type of wettability states in estuarine sandstones. The spatial distribution of oil-wet mineral abundance, calculated as the sum total of calcite, dolomite, kaolinite, hematite, and Fe-rich chlorite abundance (after Barclay and Worden [2000]), are presented in Tables 1 and 2 and Figures 15G, H and 16. Results show that the mud flats and mixed flats contain the highest abundance of oil-wet minerals in the primary depositional environment. We acknowledge that wettability state may alter during burial diagenesis (e.g., extensive quartz cementation and the illitization of kaolinite and dioctahedral smectite may lead to sandstones becoming more water wet with time).

CONCLUSIONS

This study has revealed the dominant controls on compositional variation in modern estuarine sands. Key findings of this research may be used, by analogy, to better predict the distribution of primary depositional minerals and burial diagenetic pathways in sandstone reservoirs. The main conclusions are summarized below.

1. The Ravenglass Estuary is composed of arkosic to subarkosic sediments, which reflects the drainage of the major underlying lithologies, namely Eskdale Intrusions, Borrowdale Volcanic Group, and Sherwood Sandstone Group.
2. The clay mineral assemblage of the Ravenglass Estuary is dominated by Fe–Mg-rich and well-crystalline illite, derived primarily from the glacial till. Chlorite lithics are relatively abundant in coarser-grained sediment, likely derived from pyroxene pseudomorphs in the Borrowdale Volcanic Group and chloritized mafic silicates in the Eskdale Intrusions.
3. Quartz abundance typically increases with increasing grain size up to a critical grain-size threshold of upper fine sand (177 μm); sediment coarser than 177 μm has relatively high and uniform quartz abundance. Plagioclase and carbonate abundance typically decrease with increasing grain size, with a critical grain-size threshold of lower fine sand (125 μm); sediment that is coarser than 125 μm typically has a relatively low abundance of

plagioclase and carbonate. The K-feldspar abundance is generally uniformly distributed, with a slight depletion in sediment with a grain size coarser than lower medium sand (350 μm). Clay-size fraction and kaolinite abundance decrease with increasing grain size, with a critical grain-size threshold of upper fine sand (177 μm). In sediment that is coarser than lower very fine sand (88 μm), there is a sharp decrease in chlorite and illite abundance. It is noteworthy that high chlorite concentrations, present as lithic fragments, may also occur in some foreshore, tidal inlet, tidal dune, and tidal bar sediments.

4. Mineral distribution patterns in the Ravenglass Estuary are primarily controlled by the grain size of specific minerals and estuarine hydrodynamics. The grain sizes of specific minerals are controlled by the mineral's strength and history of abrasion (e.g., glacial comminution). Provenance signals present in fluvial sediments (e.g., chlorite- and feldspar-rich River Esk sediments) are lost by intense estuarine mixing once sediment has been transported past the fluvial-marine interface.
5. This study has shown that the distribution of primary depositional mineralogy (in terms of QFL-C) may be predicted as a function of depositional environment and mean grain size. As a result, with knowledge of burial diagenetic pathways, this study may be used, by analogy, to facilitate the spatial prediction of sandstone composition and reservoir quality in similar estuarine sandstones.

REFERENCES CITED

Aagaard, P., J. S. Jahren, A. O. Harstad, O. Nilsen, and M. Ramm, 2000, Formation of grain-coating chlorite in sandstones. Laboratory synthesized *vs.* natural occurrences: *Clay Minerals*, v. 35, no. 1, p. 261–269, doi:10.1180/000985500546639.

Ajdkiewicz, J. M., and R. H. Lander, 2010, Sandstone reservoir quality prediction: The state of the art: *AAPG Bulletin*, v. 94, no. 8, p. 1083–1091, doi:10.1306/intro060110.

Ajdkiewicz, J. M., and R. E. Larese, 2012, How clay grain coats inhibit quartz cement and preserve porosity in deeply buried sandstones: Observations and experiments: *AAPG Bulletin*, v. 96, no. 11, p. 2091–2119, doi:10.1306/02211211075.

Armynot du Châtelet, E., V. Bout-Roumazielles, R. Coccioni, F. Frontalini, F. Francescangeli, G. Margaritelli, R. Rettori, F. Spagnoli, F. Semprucci, and A. Trentesaux, 2016,

Environmental control on a land-sea transitional setting: Integrated sedimentological, geochemical and faunal approaches: *Environmental Earth Sciences*, v. 75, no. 2, p. 123, doi:10.1007/s12665-015-4957-7.

Assinder, D. J., M. Kelly, and S. R. Aston, 1985, Tidal variations in dissolved and particulate phase radionuclide activities in the Esk Estuary, England, and their distribution coefficients and particulate activity fractions: *Journal of Environmental Radioactivity*, v. 2, no. 1, p. 1–22, doi:10.1016/0265-931X(85)90022-0.

Barclay, S. A., and R. H. Worden, 2000, Effects of reservoir wettability on quartz cementation in oil fields, in R. H. Worden and S. Morad, eds., *Quartz cementation in sandstones: International Association of Sedimentologists Special Publication 29*, p. 103–118, doi:10.1002/9781444304237.ch8.

Beard, D. C., and P. K. Weyl, 1973, Influence of texture on porosity and permeability of unconsolidated sand: *AAPG Bulletin*, v. 57, no. 2, p. 349–369.

Berner, E. K., and R. A. Berner, 2012, *Global environment: Water, air and geochemical cycles*, 2nd ed.: Princeton, New Jersey, Princeton University Press, 444 p.

Bloch, S., 1991, Empirical prediction of porosity and permeability in sandstones: *AAPG Bulletin*, v. 75, p. 1145–1160.

Bloch, S., R. H. Lander, and L. Bonnell, 2002, Anomalous high porosity and permeability in deeply buried sandstone reservoirs: Origin and predictability: *AAPG Bulletin*, v. 86, no. 2, p. 301–328.

Blott, S. J., and K. Pye, 2001, GRADISTAT: A grain size distribution and statistics package for the analysis of unconsolidated sediments: *Earth Surface Processes and Landforms*, v. 26, no. 11, p. 1237–1248, doi:10.1002/esp.261.

Borchers, A., I. Voigt, G. Kuhn, and B. Diekmann, 2011, Mineralogy of glaciomarine sediments from the Prydz Bay-Kerguelen region: Relation to modern depositional environments: *Antarctic Science*, v. 23, no. 2, p. 164–179, doi:10.1017/S0954102010000830.

Bousher, A., 1999, Ravenglass Estuary: Basic characteristics and evaluation of restoration options: *Restrad-Td*.

Bout-Roumazielles, V., A. Riboulleau, E. A. Châtelet, L. Lorenzoni, N. Tribouvillard, R. W. Murray, F. Müller-Karger, and Y. M. Astor, 2013, Clay mineralogy of surface sediments as a tool for deciphering river contributions to the Cariaco Basin (Venezuela): *Journal of Geophysical Research. Oceans*, v. 118, no. 2, p. 750–761, doi:10.1002/jgrc.20079.

Boyle, E., R. Collier, A. T. Dengler, J. M. Edmond, A. C. Ng, and R. F. Stallard, 1974, On the chemical mass-balance in estuaries: *Geochimica et Cosmochimica Acta*, v. 38, no. 11, p. 1719–1728, doi:10.1016/0016-7037(74)90188-4.

Boyle, E. A., J. M. Edmond, and E. R. Sholkovitz, 1977, The mechanism of iron removal in estuaries: *Geochimica et Cosmochimica Acta*, v. 41, no. 9, p. 1313–1324, doi:10.1016/0016-7037(77)90075-8.

Brockamp, O., and M. Zuther, 2004, Changes in clay mineral content of tidal flat sediments resulting from dike

- 1349 construction along the Lower Saxony coast of the North
1350 Sea, Germany: *Sedimentology*, v. 51, no. 3, p. 591–600,
1351 doi:10.1111/j.1365-3091.2004.00637.x.
- 1352 Caracciolo, L., H. Von Eynatten, R. Tolosana-Delgado,
1353 S. Critelli, P. Manetti, and P. Marchev, 2012, Petrolog-
1354 ical, geochemical, and statistical analysis of Eocene–
1355 Oligocene sandstones of the Western Thrace Basin,
1356 Greece and Bulgaria: *Journal of Sedimentary Research*,
1357 v. 82, no. 7, p. 482–498, doi:10.2110/jsr.2012.31.
- 1358 Carr, A. P., and M. W. L. Blackley, 1986, Implications of
1359 sedimentological and hydrological processes on the dis-
1360 tribution of radionuclides: The example of a salt marsh
1361 near Ravenglass, Cumbria: *Estuarine, Coastal and Shelf
1362 Science*, v. 22, no. 5, p. 529–543, doi:10.1016/0272-
1363 7714(86)90012-0.
- 1364 Chamley, H., 1989, *Clay sedimentology*: Springer-Verlag. **Q:31**
doi:10.1007/978-3-642-85916-8.
- 1366 Choquette, P. W., and L. Pray, 1970, Geologic nomenclature
1367 and classification of porosity in sedimentary carbonates:
1368 AAPG Bulletin, v. 54, no. 2, p. 207–250.
- 1369 Chuhan, F. A., K. Bjorlykke, and C. J. Lowrey, 2001, Closed-
1370 system burial diagenesis in reservoir sandstones: Exam-
1371 ples from the Garn Formation at Haltenbanken area,
1372 offshore mid-Norway: *Journal of Sedimentary Research*,
1373 v. 71, no. 1, p. 15–26, doi:10.1306/041100710015.
- 1374 Chung, F. H., 1974a, Quantitative interpretation of x-ray
1375 diffraction patterns of mixtures: I. Matrix-flushing method
1376 for quantitative multicomponent analysis: *Journal of
1377 Applied Crystallography*, v. 7, no. 6, p. 519–525, doi:
1378 10.1107/S0021889874010375.
- 1379 Chung, F. H., 1974b, Quantitative interpretation of x-ray
1380 diffraction patterns of mixtures: II. Adiabatic principle
1381 of x-ray diffraction analysis of mixtures: *Journal of Ap-
1382 plied Crystallography*, v. 7, no. 6, p. 526–531, doi:
1383 10.1107/S0021889874010387.
- 1384 Crocker, M. E., and L. M. Marchin, 1988, Wettability and
1385 adsorption characteristics of crude-oil asphaltene and
1386 polar fractions: *Journal of Petroleum Technology*, v. 40,
1387 no. 4, p. 470–474, doi:10.2118/14885-PA.
- 1388 Dalland, A., E. W. Mearns, and J. J. McBride, 1995, The
1389 application of samarium-neodymium (Sm-Nd) prove-
1390 nance ages to correlation of biostratigraphically barren
1391 strata: A case study of the Statfjord Formation in the
1392 Gullfaks Oilfield, Norwegian North Sea, in R. E. Dunay
1393 and E. A. Hailwood, eds., *Non-biostratigraphical methods
1394 of dating and correlation*: Geological Society, London,
1395 Special Publications 1995, v. 89, p. 201–222, doi:10.1144
1396 /GSL.SP.1995.089.01.10.
- 1397 Dalrymple, R. W., B. A. Zaitlin, and R. Boyd, 1992, Estuarine
1398 facies models: Conceptual models and stratigraphic im-
1399 plications: *Journal of Sedimentary Petrology*, v. 62, no. 6,
1400 p. 1130–1146, doi:10.1306/D4267A69-2B26-11D7-
1401 8648000102C1865D.
- 1402 Daneshvar, E., 2015, Dissolved iron behavior in the Rav-
1403 englass Estuary waters, an implication on the early dia-
1404 genesis: *Universal Journal of Geoscience*, v. 3, no. 1,
1405 p. 1–12, doi:10.13189/ujg.2015.030101.
- 1406 Daneshvar, E., and R. H. Worden, 2018, Feldspar alteration
1407 and Fe minerals: Origin, distribution and implications for
sandstone reservoir quality in estuarine sediments, in
P. J. Armitage, A. R. Butcher, J. M. Churchill,
A. E. Csoma, C. Hollis, R. H. Lander, J. E. Omma, and
R. H. Worden, eds., *Reservoir quality of clastic and
carbonate rocks: Analysis, modelling and prediction*:
Geological Society, London, Special Publications 2018,
v. 435, p. 123–139, doi:10.1144/SP435.17. **Q:32**
- Dickinson, W. R., and C. A. Suczek, 1979, Plate tectonics
and sandstone compositions: *AAPG Bulletin*, v. 63,
no. 12, p. 2164–2182.
- Dowey, P. J., D. M. Hodgson, and R. H. Worden, 2012, Pre-
requisites, processes, and prediction of chlorite grain
coatings in petroleum reservoirs: A review of subsurface
examples: *Marine and Petroleum Geology*, v. 32, no. 1,
p. 63–75, doi:10.1016/j.marpetgeo.2011.11.007.
- Dutton, S. P., and R. G. Loucks, 2010, Diagenetic controls
on evolution of porosity and permeability in lower
Tertiary Wilcox sandstones from shallow to ultradeep
(200–6700 m) burial, Gulf of Mexico Basin, U.S.A.:
Marine and Petroleum Geology, v. 27, no. 1, p. 69–81,
doi:10.1016/j.marpetgeo.2009.08.008.
- Ehrenberg, S. N., 1993, Preservation of anomalously high
porosity in deeply buried sandstones by grain-coating
chlorite: Examples from the Norwegian continental shelf:
AAPG Bulletin, v. 77, no. 7, p. 1260–1286.
- Esquevin, J., 1969, Influence de la composition chimique des
illites sur leur cristallinité [in French]: *Bulletin Centre
Recherche Elf Pau-SNPA*, v. 3, p. 147–153. **Q:33**
- Field, M. E., and O. H. Pilkey, 1969, Feldspar in Atlantic
continental margin sands off the southeastern United
States: *Geological Society of America Bulletin*, v. 80,
no. 10, p. 2097–2102, doi:10.1130/0016-7606(1969)80
[2097:FIACMS]2.0.CO;2.
- Folk, R. L., 1954, The distinction between grain size and
mineral composition in sedimentary-rock nomenclature:
The Journal of Geology, v. 62, no. 4, p. 344–359, doi:
10.1086/626171.
- Folk, R. L., 1968, *Petrology of sedimentary rocks*: Austin,
Texas, Hemphill Publishing. **Q:34**
- Folk, R. L., and W. C. Ward, 1957, Brazos river bar: A study
in the significance of grain size parameters: *Journal
of Sedimentary Petrology*, v. 27, no. 1, p. 3–26, doi:
10.1306/74D70646-2B21-11D7-8648000102C1865D.
- Garzanti, E., S. Andò, and G. Vezzoli, 2009, Grain-size de-
pendence of sediment composition and environmental
bias in provenance studies: *Earth and Planetary Science
Letters*, v. 277, no. 3–4, p. 422–432, doi:10.1016
/j.epsl.2008.11.007.
- Gingele, F. X., P. De Deckker, and C.-D. Hillenbrand, 2001,
Clay mineral distribution in surface sediments between
Indonesia and NW Australia—Source and transport by
ocean currents: *Marine Geology*, v. 179, no. 3–4,
p. 135–146, doi:10.1016/S0025-3227(01)00194-3.
- Glasmann, J. R., P. D. Lundegard, R. A. Clark, B. K. Penny,
and I. D. Collins, 1989, Geochemical evidence for
the history of diagenesis and fluid migration: Brent
Sandstone, Heather Field, North Sea: *Clay Minerals*,
v. 24, no. 2, p. 255–284, doi:10.1180/claymin.1989
.024.2.10. **Q:35**

- 1467 Griffiths, J., D. R. Faulkner, A. P. Edwards, and R. H. Worden, 2018, Deformation band development as a function of
1468 intrinsic host-rock properties in Triassic Sherwood
1469 Sandstone, *in* P. J. Armitage, A. R. Butcher, J. M. Churchill,
1470 A. E. Csoma, C. Hollis, R. H. Lander, J. E. Omma, and
1471 R. H. Worden, eds., Reservoir quality of clastic and
1472 carbonate rocks: Analysis, modelling and prediction:
1473 Geological Society, London, Special Publications 2018,
1474 v. 435, p. 161–176, doi:10.1144/SP435.11.
- Q:35** Grim, R. E., R. H. Bray, and W. F. Bradley, 1937, The mica
1476 in argillaceous sediments: *American Mineralogist*, v. 22,
1477 p. 813–829.
- 1478 Hillier, S., 1994, Pore-lining chlorites in siliciclastic reservoir
1479 sandstones: Electron microprobe, SEM and XRD data,
1480 and implications for their origin: *Clay Minerals*, v. 29,
1481 no. 4, p. 665–679, doi:10.1180/claymin.1994.029.4.20.
- 1482 Hillier, S., 2000, Accurate quantitative analysis of clay
1483 and other minerals in sandstones by XRD: Comparison
1484 of a Rietveld and a reference intensity ratio (RIR)
1485 method and the importance of sample preparation:
1486 *Clay Minerals*, v. 35, no. 1, p. 291–302, doi:10.1180
1487 /000985500546666.
- 1488 Hillier, S., 2003, Quantitative analysis of clay and other
1489 minerals in sandstones by x-ray powder diffraction
1490 (XRPD), *in* R. H. Worden and S. Morad, eds., Clay
1491 mineral cements in sandstones: International Association
1492 of Sedimentologists Special Publication 34, p. 213–252.
- Q:36** Kantorowicz, J. D., I. D. Bryant, and J. M. Dawans, 1987,
1494 Controls on the permeability and distribution of car-
1495 bonate cements in Jurassic sandstones: Bridgeport Sands,
1496 southern England, and Viking Group, Troll field,
1497 Norway, *in* J. D. Marshall, ed., Diagenesis of sedimentary
1498 sequences: Geological Society, London, Special Publica-
1499 tions 1987, v. 36, p. 103–118.
- Q:37** Kelly, M., M. Emptage, S. Mudge, K. Bradshaw, and
1501 J. Hamilton-Taylor, 1991, The relationship between
1502 sediment and plutonium budgets in a small macrotidal
1503 estuary: Esk Estuary, Cumbria, UK: *Journal of Environ-
1504 mental Radioactivity*, v. 13, no. 1, p. 55–74, doi:
1505 10.1016/0265-931X(91)90039-I.
- 1506 Ketzer, J. M., M. Holz, S. Morad, and I. Al-Aasm, 2003,
1507 Sequence stratigraphic distribution of diagenetic alter-
1508 ations in coal-bearing, paralic sandstones: Evidence from
1509 the Rio Bonito Formation (early Permian), southern Brazil:
1510 *Sedimentology*, v. 50, no. 5, p. 855–877, doi:10.1046
1511 /j.1365-3091.2003.00586.x.
- 1512 Kübler, B., 1964, Les argiles, indicateurs de métamorphisme
1513 [in French]: *Revue de l'Institut Français du Pétrole*, v. 19,
1514 p. 1093–1112.
- 1515 Lloyd, J. M., Y. Zong, P. Fish, and J. B. Innes, 2013, Holocene
1516 and lateglacial relative sea-level change in north-west
1517 England: Implications for glacial isostatic adjustment
1518 models: *Journal of Quaternary Science*, v. 28, no. 1,
1519 p. 59–70, doi:10.1002/jqs.2587.
- 1520 Matlack, K. S., D. W. Houseknecht, and K. R. Applin, 1989,
1521 Emplacement of clay into sand by infiltration: *Journal of
1522 Sedimentary Petrology*, v. 59, p. 77–87.
- 1523 McDougall, D. A., 2001, The geomorphological impact of
1524 Loch Lomond (Younger Dryas) Stadial plateau icefields
1525 in the central Lake District, northwest England: *Journal
1526 of Quaternary Science*, v. 16, no. 6, p. 531–543, doi:
1527 10.1002/jqs.624.
- 1528 Merritt, J. W., and C. A. Auton, 2000, An outline of the
1529 lithostratigraphy and depositional history of Quaternary
1530 deposits in the Sellafeld district, west Cumbria: *Pro-
1531 ceedings of the Yorkshire Geological Society*, v. 53, no. 2,
1532 p. 129–154, doi:10.1144/pygs.53.2.129.
- 1533 Meyer, E. E., G. W. Greene, N. A. Alcantar, J. N. Israelachvili,
1534 and J. R. Boles, 2006, Experimental in situ study of
1535 the dissolution of quartz by a muscovite brine: Implica-
1536 tions for pressure solution: *Journal of Metamorphic and
1537 Physical Research. Solid Earth*, v. 111, p. 107–120, doi:
1538 /2005JB004010.
- 1539 Moore, D. M., and R. C. Reynolds, Jr., 1997, X-ray
1540 diffraction and the identification and analysis of clay
1541 minerals: *Clay Minerals Society, London, UK: Blackwell
1542 Science, Oxford*, 378 p.
- 1543 Morad, S., K. Al-Ramadan, J. M. Ketzer, and L. F. de Ros,
1544 2010, The impact of diagenesis on the heterogeneity of
1545 sandstone reservoirs: A review of the role of depositional
1546 facies and sequence stratigraphy: *AAPG Bulletin*, v. 94,
1547 no. 8, p. 1267–1309, doi:10.1306/04211009178.
- 1548 Morad, S., L. F. de Ros, J. P. Nystuen, and M. Bergan, 1998,
1549 Carbonate diagenesis and porosity evolution in sheet-
1550 flood sandstones: Evidence from the Middle and Lower
1551 Lunde Members (Triassic) in the Snorre Field, Norwegian
1552 North Sea, *in* S. Morad, ed., Carbonate cementation
1553 in sandstones: Distribution patterns and geochemical
1554 evolution: International Association of Sedimentolo-
1555 gists Special Publication 26, p. 53–85, doi:10.1002
1556 /9781444304893.ch3.
- Q:39** Morad, S., J. M. Ketzer, and L. F. de Ros, 2000, Spatial and
1557 temporal distribution of diagenetic alterations in silici-
1558 clastic rocks: Implications for mass transfer in sediment-
1559 ary basins: *Sedimentology*, v. 47, p. 95–120, doi:
1560 10.1046/j.1365-3091.2000.00007.x.
- 1561 Morad, S., J. M. Ketzer, and L. F. de Ros, 2012, Linking
1562 diagenesis to sequence stratigraphy: International Associo-
1563 tion of Sedimentologists Special Publication 45.
- Q:40** Morris, J. E., G. J. Hampson, and H. D. Johnson, 2006, A
1565 sequence stratigraphic model for an intensely bioturbated
1566 shallow-marine sandstone: The Bridport Sand Forma-
1567 tion, Wessex Basin, UK: *Sedimentology*, v. 53, no. 6,
1568 p. 1229–1263, doi:10.1111/j.1365-3091.2006.00811.x.
- 1569 Moseley, F., 1978, The geology of the Lake District: Yorkshire
1570 Geological Society.
- Q:41** Odeh, R. E., and J. O. Evans, 1974, Algorithm AS 70: The
1572 percentage points of the normal distribution: *Journal of
1573 the Royal Statistical Society. Series C, Applied Statistics*,
1574 v. 23, p. 96–97.
- 1575 Odom, I. E., T. W. Doe, and R. H. Dott, 1976, Nature
1576 of feldspar-grain size relations in some quartz-rich
1577 sandstones: *Journal of Sedimentary Research*, v. 46,
1578 p. 862–870.
- 1579 Oelkers, E. H., P. A. Bjorkum, and W. M. Murphy, 1996,
1580 A petrographic and computational investigation of
1581 quartz cementation and porosity reduction in North Sea
1582 sandstones: *American Journal of Science*, v. 296, no. 4,
1583 p. 420–452, doi:10.2475/ajs.296.4.420.
- 1584

Note that page ranges
are now not normally
listed for papers
published in the
Journal of
Geophysical
Research

- 1585 Oliveira, A., F. Rocha, A. Rodrigues, J. Jouanneau, A. Dias, 1644
 1586 O. Weber, and C. Gomes, 2002, Clay minerals from the 1645
 1587 sedimentary cover from the Northwest Iberian shelf: 1646
 1588 Progress in Oceanography, v. 52, no. 2–4, p. 233–247, 1647
 1589 doi:10.1016/S0079-6611(02)00008-3. 1648
- 1590 Primmer, T. J., C. A. Cade, J. Evans, J. G. Gluyas, M. S. Hopkins, 1649
 1591 N. H. Oxtoby, P. C. Smalley, E. A. Warren, and 1650
 1592 R. H. Worden, 1997, Global patterns in sandstone dia- 1651
 1593 genesis: Their application to reservoir quality prediction 1652
 1594 for petroleum exploration, in J. A. Kupecz, J. Gluyas, and 1653
 1595 S. Bloch, eds., Reservoir quality prediction in sandstones 1654
 1596 and carbonates: AAPG Memoir 69, p. 61–78. 1655
- 1597 Quirke, J., C. M. B. Henderson, R. A. D. Patrick, K. M. Rosso, 1656
 1598 A. Dent, J. W. Sharples, and C. I. Pearce, 2015, Char- 1657
 1599 acterizing mineralogy and redox reactivity in potential 1658
 1600 host rocks for a UK geological disposal facility: Miner- 1659
 1601 alogical Magazine, v. 79, no. 6, p. 1353–1367, doi: 1660
 1602 10.1180/minmag.2015.079.6.11. 1661
- 1603 R Core Team, 2016, R: A language and environment for 1662
 1604 statistical computing: Vienna, Austria, R Foundation 1663
 1605 for Statistical Computing. 1664
- 1606 Ramm, M., and K. Bjorlykke, 1994, Porosity/depth trends in 1665
 1607 reservoir sandstones: Assessing the quantitative effects of 1666
 1608 varying pore-pressure, temperature history and miner- 1667
 1609 alogy, Norwegian shelf data: Clay Minerals, v. 29, 1668
 1610 p. 475–490, doi:10.1180/claymin.1994.029.4.07. 1669
- 1611 Ramm, M., A. W. Forsberg, and J. Jahren, 1997, Porosity- 1670
 1612 depth trends in deeply buried Upper Jurassic reservoirs 1671
 1613 in the Norwegian Central Graben: An example of porosity 1672
 1614 preservation beneath the normal economic basement by 1673
 1615 grain-coating microquartz, in J. A. Kupecz, J. Gluyas, and 1674
 1616 S. Bloch, eds., Reservoir quality prediction in sandstones 1675
 1617 and carbonates: AAPG Memoir 69, p. 177–200. 1676
- 1618 Rawling, G. C., and L. B. Goodwin, 2003, Cataclasis and 1677
 1619 particulate flow in faulted, poorly lithified sediments: 1678
 1620 Journal of Structural Geology, v. 25, no. 3, p. 317–331, 1679
 1621 doi:10.1016/S0191-8141(02)00041-X. 1680
- 1622 Rider, M., and M. Kennedy, 2011, The geological interpre- 1681
 1623 tation of well logs: Cambridge, Rider-French Consulting, 1682
 1624 440 p. 1683
- 1625 Saiag, J., B. Brigaud, E. Portier, G. Desaubliaux, A. Bucherie, 1684
 1626 S. Miska, and M. Pagel, 2016, Sedimentological control 1685
 1627 on the diagenesis and reservoir quality of tidal sandstones 1686
 1628 of the Upper Cape Hay Formation (Permian, Bonaparte 1687
 1629 Basin, Australia): Marine and Petroleum Geology, v. 77, 1688
 1630 p. 597–624, doi:10.1016/j.marpetgeo.2016.07.002. 1689
- 1631 Scherer, M., 1987a, Erratum to “Parameters influencing po- 1690
 1632 rosity in sandstones: A model for sandstone porosity 1691
 1633 prediction” [AAPG Bulletin, v. 71, no. 5, p. 485–491]: 1692
 1634 AAPG Bulletin, v. 71, no. 12, p. 1508, doi:10.1306 1693
 1635 /703C80FB-1707-11D7-8645000102C1865D. 1694
- 1636 Scherer, M., 1987b, Parameters influencing porosity in sand- 1695
 1637 stones: A model for sandstone porosity prediction: AAPG 1696
 1638 Bulletin, v. 71, no. 5, p. 485–491. 1697
- 1639 Schmid, S., R. H. Worden, and Q. J. Fisher, 2006, Sedi- 1698
 1640 mentary facies and the context of dolomite in the 1699
 1641 Lower Triassic Sherwood Sandstone Group: Corrib Field 1700
 1642 west of Ireland: Sedimentary Geology, v. 187, no. 3–4, 1701
 1643 p. 205–227, doi:10.1016/j.sedgeo.2005.12.028. 1702
- Sholkovitz, E. R., 1978, The flocculation of dissolved Fe, Mn, 1644
 Al, Cu, Ni, Co and Cd during estuarine mixing: Earth and 1645
 Planetary Science Letters, v. 41, no. 1, p. 77–86, doi: 1646
 10.1016/0012-821X(78)90043-2. 1647
- Sholkovitz, E. R., E. A. Boyle, and N. B. Price, 1978, The 1648
 removal of dissolved humic acids and iron during es- 1649
 tuarine mixing: Earth and Planetary Science Letters, 1650
 v. 40, no. 1, p. 130–136, doi:10.1016/0012-821X(78) 1651
 90082-1. 1652
- Stevens, R. L., 1991, Grain-size distribution of quartz and 1653
 feldspar extracts and implications for flocculation pro- 1654
 cesses: Geo-Marine Letters, v. 11, no. 3–4, p. 162–165, 1655
 doi:10.1007/BF02431004. 1656
- Stricker, S., and S. J. Jones, 2018, Enhanced porosity pres- 1657
 ervation by pore fluid overpressure and chlorite grain 1658
 coatings in the Triassic Skagerrak, Central Graben, North 1659
 Sea, UK, in P. J. Armitage, A. R. Butcher, J. M. Churchill, 1660
 A. E. Csoma, C. Hollis, R. H. Lander, J. E. Omma, and 1661
 R. H. Worden, eds., Reservoir quality of clastic and 1662
 carbonate rocks: Analysis, modelling and prediction: 1663
 Geological Society, London, Special Publications 2018, 1664
 v. 435, p. SP435-4. 1665
- Stricker, S., S. J. Jones, S. Sathar, L. Bowen, and N. Oxtoby, 1666
 2016, Exceptional reservoir quality in HPHT reservoir 1667
 settings: Examples from the Skagerrak Formation of the 1668
 Heron Cluster, North Sea, UK: Marine and Petroleum 1669
 Geology, v. 77, p. 198–215, doi:10.1016/j.marpetgeo 1670
 .2016.02.003. 1671
- Trewin, N. H., and A. E. Fallick, 2009, Quartz cement origins 1672
 and budget in the Tumblagooda Sandstone, western 1673
 Australia, in R. H. Worden and S. Morad, eds., Quartz 1674
 cementation in sandstones: International Association of 1675
 Sedimentologists Special Publication 29, p. 219–229. 1676
- Walderhaug, O., 1994a, Precipitation rates for quartz cement 1677
 in sandstones determined by fluid-inclusion micro- 1678
 thermometry and temperature-history modeling: Journal 1679
 of Sedimentary Research, Section A, Sedimentary Pe- 1680
 trology and Processes, v. 64, p. 324–333. 1681
- Walderhaug, O., 1994b, Temperatures of quartz cementation 1682
 in Jurassic sandstones from the Norwegian continental 1683
 shelf—Evidence from fluid inclusions: Journal of Sedi- 1684
 mentary Research, Section A, Sedimentary Petrology and 1685
 Processes, v. 64, p. 311–323. 1686
- Watson, D. F., and G. M. Philip, 1985, Comment on “A 1687
 nonlinear empirical prescription for simultaneously in- 1688
 terpolating and smoothing contours over an irregular 1689
 grid” by F. Duggan: Computer Methods in Applied 1690
 Mechanics and Engineering, v. 50, p. 195–198. 1691
- Weltje, G. J., 2006, Ternary sandstone composition and 1692
 provenance: An evaluation of the ‘Dickinson model’, 1693
 in A. Bucciati, G. Mateu-Figueras, and V. Pawlowsky- 1694
 Glahn, eds., Compositional data analysis in the ge- 1695
 sciences: From theory to practice: Geological Society, 1696
 London, Special Publications 2006, v. 264, no. 1, p. 79–99, 1697
 doi:10.1144/GSL.SP.2006.264.01.07. 1698
- Wooldridge, L. J., R. H. Worden, J. Griffiths, A. Thompson, 1699
 and P. Chung, 2017a, Biofilm origin of clay-coated sand 1700
 grains: Geology, v. 45, no. 10, p. 875–878, doi:10.1130 1701
 /G39161.1. 1702

Q:42

Q:45

Q:46

Q:44

Q:45

Q:46

Q:47

1703
1704
1705
1706
1707
1708
1709
1710
1711
1712
1713
1714
1715
1716
1717
1718
1719
1720
1721
1722
1723
1724
1725
1726
1727
1728
1729
1730

Wooldridge, L. J., R. H. Worden, J. Griffiths, and J. E. P. Utley, 2017b, Clay-coated sand grains in petroleum reservoirs: Understanding their distribution via a modern analogue: *Journal of Sedimentary Research*, v. 87, no. 4, p. 338–352, doi:10.2110/jsr.2017.20.

Wooldridge, L. J., R. H. Worden, J. Griffiths, J. E. P. Utley, and A. Thompson, 2018, The origin of clay-coated sand grains and sediment heterogeneity in tidal flats: *Sedimentary Geology*, v. 373, p. 191–209, doi:10.1016/j.sedgeo.2018.06.004.

Worden, R. H., 2006, Dawsonite cement in the Triassic Lam Formation, Shabwa Basin, Yemen: A natural analogue for a potential mineral product of subsurface CO₂ storage for greenhouse gas reduction: *Marine and Petroleum Geology*, v. 23, no. 1, p. 61–77, doi:10.1016/j.marpetgeo.2005.07.001.

Worden, R. H., P. J. Armitage, A. R. Butcher, J. M. Churchill, A. E. Csoma, C. Hollis, R. H. Lander, and J. E. Omma, 2018, Petroleum reservoir quality prediction: Overview and contrasting approaches from sandstone and carbonate communities, in P. J. Armitage, A. R. Butcher, J. M. Churchill, A. E. Csoma, C. Hollis, R. H. Lander, J. E. Omma, and R. H. Worden, eds., *Reservoir quality of clastic and carbonate rocks: Analysis, modelling and prediction*: Geological Society, London, Special Publications 2018, v. 435, p. 1–31.

Worden, R. H., and S. D. Burley, 2003, Sandstone diagenesis: The evolution from sand to stone, in R. H. Worden

and S. D. Burley, eds., *Sandstone diagenesis: Recent and ancient*, International Association of Sedimentologists Reprint Series 4, p. 3–44, doi:10.1002/9781444304459.ch.

Worden, R. H., M. J. Mayall, and I. J. Evans, 1997, Predicting reservoir quality during exploration: Lithic grains, porosity and permeability in Tertiary clastics of the South China Sea basin, in A. J. Fraser, S. J. Matthews, and R. W. Murphy, eds., *Petroleum geology of Southeast Asia*: Geological Society, London, Special Publications 1997, v. 126, p. 107–115.

Worden, R. H., M. Mayall, and I. J. Evans, 2000, The effect of ductile-lithic sand grains and quartz cement on porosity and permeability in Oligocene and lower Miocene clastics, South China Sea: Prediction of reservoir quality: *AAPG Bulletin*, v. 84, no. 3, p. 345–359, doi:10.1306/C9EBCDE7-1735-11D7-8645000102C1865D.

Worden, R. H., and S. Morad, 2003, Clay minerals in sandstones: Controls on formation, distribution and evolution, in R. H. Worden and S. Morad, eds., *Clay mineral cements in sandstones*: International Association of Sedimentologists Special Publication 34, p. 3–41.

Young, B., N. J. Fortey, and P. H. A. Nancarrow, 1986, An occurrence of tungsten mineralisation in the Eskdale Intrusion, West Cumbria: *Proceedings of the Yorkshire Geological Society*, v. 46, no. 1, p. 15–21, doi:10.1144/pygs.46.1.15.

1731
1732
1733
Q:48
1735
1736
1737
1738
1739
1740
Q:49
1742
1743
1744
1745
1746
1747
Q:50
1749
1750
1751
Q:51
1754
1755
1756
1757
1758

AUTHOR QUERIES

AUTHOR PLEASE ANSWER ALL QUERIES

1

- Q:1 Please confirm the short title on the bottom of page 2: "Compositional Variation in Modern Estuarine Sands"
- Q:2 In the affiliations, please confirm: are "BP Exploration" and "BP Upstream Technology" separate companies/institutions, or should these be treated as departments within BP?
- Q:3 In the sentence beginning "James E. P. Utley is...," please confirm the edit preserves your intent or amend as needed.
- Q:4 Please spell out CASP in the bio for author Duller.
- Q:5 In the sentence beginning "Special thanks are...," please confirm that "Thermo Fisher Scientific" is correct or amend as needed.
- Q:6 In the sentence beginning "The composition of sandstone is...," please check the phrase "all the processes active between the sediment source area and the final site of deposition" and revise for clarity if necessary.
- Q:7 In the sentence beginning "The composition of sandstone...," please confirm that the edits preserve your intent or amend as needed.
- Q:8 Per journal style, "sedimentary rocks" is preferable over "sediments" if rocks are being referred to. Please check the use of "sediments" throughout and amend if needed.
- Q:9 In the sentence beginning "Clay-rich ductile versus...," please confirm that "phyllosilicate lithic- and mica-rich sediments" is correct or amend as needed.
- Q:10 Please provide an English unit conversion for ">7 m" in the sentence beginning "The Ravenglass Estuary is a shallow..."
- Q:11 In the sentence beginning "Mean grain size (microns)...," please spell out "σg."
- Q:12 If appropriate, please create a reference for "International Centre for Diffraction Data Powder Diffraction File-2008" and cite it in the sentence beginning "Mineralogy was determined by..."
- Q:13 In the sentence beginning "The Esquevin index, which has...," "Du Chatelet et al. 2016" has been changed to "Armynot du Châtelet et al. 2016" to match the reference list. Please confirm or amend as needed.
- Q:14 In the sentence beginning "To establish illite crystallinity...," please clarify "001." Should there be a unit of measure associated with this?
- Q:15 Please check the sentence beginning "Mineralogy of different..." and confirm the edits preserve your intent or amend as needed.
- Q:16 In the sentence beginning "It is important to note...," please confirm that "SEM-EDS" has been expanded correctly or amend as needed.

AUTHOR QUERIES

AUTHOR PLEASE ANSWER ALL QUERIES

2

- Q:17 In the sentence beginning "The SEM-EDS system...", "EDS-SEM" was changed to "SEM-EDS," as the latter was used predominantly. Please confirm or amend as needed.
- Q:18 In the sentence beginning "Smectite abundance is negligible...", please check the phrase "size sediment fractions" and revise for clarity, if necessary.
- Q:19 Please check the sentence beginning "There is a subtle reduction..." and confirm the edits preserve your intent or amend as needed.
- Q:20 Per journal style, quotation marks should only be used to offset a quote, slang, or coined words and phrases or to define a term being used ironically or out of its normal context. Quotation marks should appear only at the first mention of such terms and be removed thereafter. This has been applied to "Dickinson model" throughout the text. Please confirm or amend as needed.
- Q:21 The in-text citation "Du Chatelet et al., 2016" is not in the reference list. Please correct the citation, add the reference to the list, or delete the citation.
- Q:22 In the sentence beginning "However, results of this study...", please check "susceptible to reduction less than 125 μm " and confirm it is correct or amend as needed.
- Q:23 In the sentence beginning "In contrast, in sediment...", please check the phrase "end to be resuspended" and revise for clarity, if necessary.
- Q:24 In the sentence beginning "In addition, petrographic QFL studies...", please check "glacial and nonglacial derived sediments." Should it be "glacier- and nonglacier-derived sediments"?
- Q:25 Please check the edits to the sentence beginning "Because mud flats..." and confirm they preserve your intent or amend as needed.
- Q:26 In the sentence beginning "As a result, better reservoir...", please check "Goldilocks" and confirm that it preserves your intent or amend as needed.
- Q:27 In the sentence beginning "Whether a reservoir rock...", please check "implication from economic viability" and revise for clarity, if necessary.
- Q:28 Please provide a full page range for Armynot du Châtelet et al. 2016 or confirm that it is an abstract.
- Q:29 Please provide a publisher location for International Association of Sedimentologists in Barclay and Worden 2000.
- Q:30 Please provide a publisher location and page count for Bousher 1999.
- Q:31 Please provide a publisher location and page count for Chamley 1989.
- Q:32 Please confirm or amend the updated information for Daneshvar and Worden 2018.

AUTHOR QUERIES

AUTHOR PLEASE ANSWER ALL QUERIES

3

- Q:33 Please expand “SNPA” in Esquevin 1969.
- Q:34 Please provide a page count for Folk 1968.
- Q:35 Please confirm or amend the updated information for Griffiths et al. 2018.
- Q:36 Please provide location of publisher (International Association of Sedimentologists) for Hillier 2003.
- Q:37 Please check the updated information for Kantorowicz et al. 1987 and confirm it is correct or amend as needed.
- Q:38 Please provide a page range for Meyer et al. 2006.
- Q:39 Please provide location of publisher (International Association of Sedimentologists) for Morad et al. 1998.
- Q:40 Please provide location of publisher (International Association of Sedimentologists) and page count for Morad et al. 2012.
- Q:41 Please provide a page count and publisher location for Moseley 1978.
- Q:42 Please provide a page count for R Core Team 2016 if appropriate.
- Q:43 Please confirm that the page count for Rider and Kennedy 2011 is correct or amend as needed.
- Q:44 Note that a corrigendum was published related to Scherer 1987, and the appropriate reference has been added here. The in-text citations have also been updated. Please confirm or amend as needed.
- Q:45 Please clarify the page count in Stricker and Jones 2016. Should it just be “4 p.”? Please also confirm the updated information.
- Q:46 Please provide location of publisher (International Association of Sedimentologists) for Trewin and Fallick 2009.
- Q:47 Please confirm or amend the updated information for Weltje 2006.
- Q:48 Please provide a publisher location for International Association of Sedimentologists in Worden and Burley 2003.
- Q:49 Please confirm or amend the updated information for Worden et al. 1997.
- Q:50 Worden et al. 2000b seemed to be a duplicate or earlier version of 2000a, so it has been deleted. Please confirm or clarify.
- Q:51 Please provide a publisher location for International Association of Sedimentologists in Worden and Morad 2003.

AUTHOR QUERIES

AUTHOR PLEASE ANSWER ALL QUERIES

4

- Q:52 Please confirm that “SEM-EDS” has been expanded correctly in the first sentence of the Figure 6 caption or amend as needed.
- Q:53 Please confirm that “Musc.” Has been expanded correctly at the end of the Figure 6 caption.
- Q:54 Please confirm that “XRD-QFL” has been expanded correctly in the first sentence of the Figure 7 caption.
- Q:55 Per journal style, all panel labels for a figure must be mentioned in its caption. Please cite panels A–D in the captions of Figures 9–12.
- Q:56 Per journal style, table titles should only be one sentence. The rest of the text appearing after the first sentence of each table title has been set as a legend beneath the table. Please confirm or amend as needed.
- Q:57 Per journal style, multi-part tables should be split into individual tables. Tables 1–3 have been split into 6 separate tables and the in-text citations have been updated. Please confirm or amend as needed.
- Q:58 For the last 3 row headings in Table 1 and Table 2, are the parenthetical values still standard deviations? If so, please indicate this in the row headings (e.g., “Mean grain size, μm (sd)”).
- Q:59 Please add dashes or other abbreviations to indicate not applicable for blank cells in Table 2 (and include definition in the Abbreviations list).
- Q:60 In the legend of Table 2, please explain the significance of “x” in the bottom-right cell. Is this meant to indicate no data?
- Q:61 In Tables 3–6, please confirm that the bold formatting has been retained correctly or amend as needed. In each legend, “Gray values” has been changed to “Nonbolded values.”
- Q:62 Please insert an en dash or some other “not applicable” indicator in the blank cells in Tables 3–6 and explain their significance in the legend of each table.
- Q:63 In the legends of Tables 3–6, please explain the significance of “X.” Is this meant to indicate no data?
-
-